# Synthesis of Vinylene-*Co,N*-Linked Multi(porphyrin)s by the Addition of Free-Base Porphyrins to a $C_2H_2$ Complex of Cobalt(III) Porphyrin and Their Oxidative Rearrangement to Vinylene-*N,N′*-Linked Multi(porphyrin)s

**Jun-ichiro Setsune,*,† Hirokazu Takeda,† Shoji Ito,† Yugo Saito,† Yoshihiro Ishimaru,† Koji Fukuhara,‡ Yasushi Saito,‡ Teijiro Kitao,‡,§ and Tomohiro Adachi||**

Department of Chemistry, Faculty of Science, Kobe University, Nada, Kobe 657, Japan, and Department of Applied Chemistry, College of Engineering, and Department of Chemistry, School of Integrated Arts and Sciences, University of Osaka Prefecture, Sakai, Osaka 591, Japan

*Received June 19, 1997*

The nucleophilic addition reaction of a pyrrole nitrogen of free-base porphyrins to a $\pi$-complexed acetylene ligand in a cationic $Co^{III}$ porphyrin intermediate afforded good yields of vinylene-*Co,N′*-linked bis(porphyrin)s, (Por)$Co^{III}$−CH═CH−(*N*-Por)$H_2$. N-substituted porphyrin free bases are N-vinylated regioselectively at the pyrrole adjacent to the original N-substituted pyrrole in this reaction. Tris- and tetrakis(porphyrin)s have been prepared by reacting a vinylene-*N,N′*-linked bis(*meso*-tetraarylporphyrin) with (OEP)$Co^{III}(H_2O)_2ClO_4$ (OEP: octaethylporphyrin dianion) and acetylene. The tetrakis(porphyrin) proved to be a 1:1 mixture of $C_i$- and $C_2$-symmetric regioisomers. These organometallic $Co^{III}$ complexes underwent facile oxidative migration of the Co-bound vinyl group to a porphyrin pyrrole nitrogen when treated with $Fe^{III}$ salts or $HClO_4$ to provide moderate to good yields of $Co^{II}$ vinylene-*N,N′*-linked multi(porphyrin) complexes. (Vinylene-*N,N′*)bis(porphyrin) free bases with combinations of different porphyrins have been obtained by this procedure. The homobinuclear ($2Co^{II}$, $2Cu^{II}$, and $2Zn^{II}$) and heterobinuclear ($Co^{II}Cu^{II}$ and $Co^{II}Zn^{II}$) complexes have been prepared and characterized spectroscopically. The single-crystal X-ray analysis of (CH═CH-*N,N′*)[(OEP)$Co^{II}$Cl][(TPP)$Zn^{II}$Cl] (TPP: *meso*-tetraphenylporphyrin dianion) showed a face-to-face structure with an average inter-ring separation of 4.39 Å (triclinic $P\bar{1}$; $Z = 2$; $a = 14.806(4)$, $b = 18.703(10)$, $c = 13.796(3)$ Å, $\alpha = 97.69(3)$, $\beta = 99.57(2)$, $\gamma = 96.74(3)°$).

## Introduction

Face-to-face porphyrin structures have recently attracted considerable attention, and their applications to bimetallic catalysts and one-dimensional conducting materials have been discussed.[1−3] Face-to-face porphyrins with covalent linkages between porphyrin nuclei are classified according to the type of linkage: (i) organic spacers covalently connected at the porphyrin periphery (*meso* or $\beta$-pyrrole);[1,4] (ii) metal−metal bonding in metalloporphyrins;[5] (iii) bridging axial ligands such as $\mu$-oxo;[6] (iv) f-block metal elements which can provide coordination sites for two porphyrins.[7] The only examples of linkages connected to pyrrole nitrogens in face-to-face porphyrin systems reported are those in which a porphyrin *N*-oxide is axially coordinated to a $Co^{III}$ or $Mn^{III}$ porphyrin by the oxygen atom.[8] As indicated by the X-ray structure of these complexes, (Por)M−O−(*N*-Por)H (M = $Co^{III}$ or $Mn^{III}$), a short spacer connected to a pyrrole nitrogen forces the two porphyrin planes to be in a face-to-face orientation. Thus, linkages connected to pyrrole nitrogens are expected to provide a convenient tool for the preparation of the face-to-face porphyrin systems,[9] if the difficulty in the N-alkylation of the porphyrin nitrogen and the unstability of the N-substituted porphyrins can be overcome.

We have recently demonstrated that acetylene is reversibly bound to (perchlorato)$Co^{III}$ porphyrins (**1**) in noncoordinating solvents such as $CH_2Cl_2$.[10] In the presence of 2,6-lutidine, unable to coordinate to the metal in a porphyrin core for steric reasons, a 2,6-lutidine nitrogen attacks the acetylene $\pi$-coordinated to the $Co^{III}$ porphyrin.[11] Thus, $\sigma$-[2-(2,6-dimethyl-1-pyridinio)vinyl]$Co^{III}$ porphyrin (**2**) is obtainable in good yields (Scheme 1). The use of a sterically hindered amine is crucial

* To whom correspondence should be addressed. E-mail: setsunej@kobe-u.ac.jp.

† Kobe University.

‡ University of Osaka Prefecture (College of Engineering).

§ Deceased January 4, 1992.

|| University of Osaka Prefecture (Faculty of Integrated Arts and Sciences); responsible for X-ray analysis.

(1) (a) Chang, C. K.; Abdalmuhdi, I. *J. Org. Chem.* **1983**, *48*, 5388−5390. (b) Abdalmuhdi, I.; Chang, C. K. *J. Org. Chem.* **1985**, *50*, 411−413. (c) Eaton, S. S.; Eaton, G. R.; Chang, C. K. *J. Am. Chem. Soc.* **1985**, *107*, 3177−3184. (d) Nagata, T.; Osuka, A.; Maruyama, K. *J. Am. Chem. Soc.* **1990**, *112*, 3054−3059. (e) Osuka, A.; Ida, K.; Maruyama, K. *Chem. Lett.* **1989**, 741−744.

(2) (a) Collman, J. P.; Wagenknecht, P. S.; Hutchison, J. E.; Lewis, N. S.; Lopez, M. A.; Guilard, R.; L'Her, M.; Bothner-By, A. A.; Mishra, P. K. *J. Am. Chem. Soc.* **1992**, *114*, 5654−5664. (b) Collman, J. P.; Ha, Y.; Wagenknecht, P. S.; Lopez, M. A.; Guilard, R. *J. Am. Chem. Soc.* **1993**, *115*, 9080−9088. (c) Collman, J. P.; Hutchison, J. E.; Lopez, M. A.; Guilard, R. *J. Am. Chem. Soc.* **1992**, *114*, 8066−8073. (d) Collman, J. P.; Hutchison, J. E.; Ennis, M. S.; Lopez, M. A.; Guilard, R. *J. Am. Chem. Soc.* **1992**, *114*, 8074−8080. (e) Guilard, R.; Brandes, S.; Tabard, A.; Bouhmaida, N.; Lecomte, C.; Richard, P.; Latour, J.-M. *J. Am. Chem. Soc.* **1994**, *116*, 10202−10211. (f) Naruta, Y.; Sasayama, M.; Sasaki, T. *Angew. Chem.* **1994**, *106*, 1964−1965. (g) Park, G. I.; Nakajima, S.; Osuka, A.; Kim, K. *Chem. Lett.* **1995**, 255−258. (h) Mackay, L. G.; Wylie, R. S.; Sanders, J. K. M. *J. Am. Chem. Soc.* **1994**, *116*, 3141−3142. (i) Collman, J. P.; McDevitt, J. T.; Leidner, C. R.; Yee, G. T.; Torrance, J. B.; Little, W. A. *J. Am. Chem. Soc.* **1987**, *109*, 4606−4614.

(3) Scheidt, W. R.; Lee, Y. J. *Structure Bonding 64*; Springer-Verlag: Berlin, Heidelberg, 1987.

S0020-1669(97)00770-2 CCC: $15.00 
Published on Web 04/11/1998

**Scheme 1**

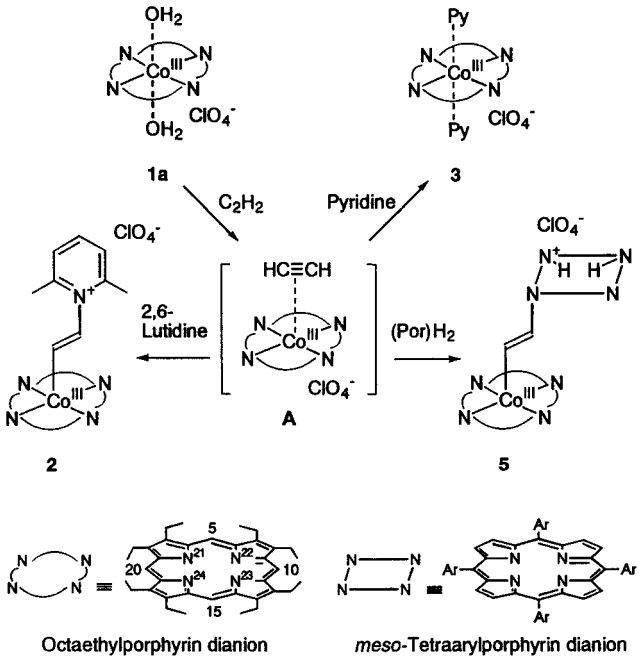


to this reaction, because unhindered amines such as pyridine preferentially coordinate to the metal replacing the acetylene ligand to give bis(amine)$Co^{III}$ porphyrin complexes (**3**). The highly cationic nature of the acetylene coordinated to a monocationic $Co^{III}$ porphyrin is expected to cause attack of a porphyrin pyrrole nitrogen, even if the nitrogen is sterically much more hindered than in 2,6-lutidine.[12]

**Scheme 2**

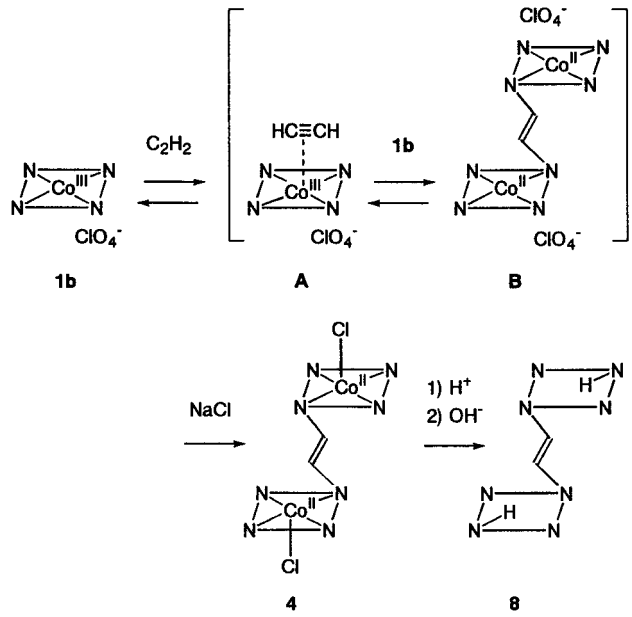


This paper shows that free-base porphyrins are effectively N-vinylated to give face-to-face bis-, tris-, and tetrakis(porphyrin)s which are linked by the vinylene-*Co,N′* linkages. The one-electron oxidation of these vinylene-*Co,N′*-linked bis(porphyrin)$Co^{III}$ complexes affords vinylene-*N,N′*-linked bis(porphyrin)s with the combination of different porphyrins. Synthesis and spectroscopic properties of the metal complexes of vinylene-*N,N′*-linked bis-(porphyrin)s are also described.

## Results and Discussion

**Vinylene-*Co,N′*-Linked Multi(porphyrin)s (5a−e, 9, 10).** We have shown that a $Co^{III}$ acetylene $\pi$-complex (**A**) is thermally in equilibrium with the (vinylene-*N,N′*)bis(porphyrin) bis-$Co^{II}$ complex (**B**) via an unusual radical mechanism in the reaction of the cationic $Co^{III}$ porphyrins (**1**) with acetylene (Scheme 2).[10] The bis(porphyrin) bis-$Co^{II}$ complexes, (CH═CH-*N,N′*)[(Por)$Co^{II}$Cl]$_2$ (**4**), were isolated and characterized when the (perchlorato)$Co^{III}$ complexes of *meso*-tetraarylporphyrins were allowed to react with acetylene and then with NaCl. Whereas this novel dimerization reaction provides a one-step synthetic method for homo dimers in moderate to good yields, it is not applicable to the case of $Co^{III}$ octaethylporphyrin. This is probably because the interaction between $Co^{II}$ and the vinylene-*N,N′* moiety which leads to decomposition is stronger in the sterically less hindered OEP dimer than in the TPP dimer. Furthermore, hetero dimers are impossible to prepare by this one-step procedure. A more versatile approach to this interesting vinylene-*N,N′*-linked bis(porphyrin) structure is possible by

(4) (a) Collman, J. P.; Chong, H. O.; Jameson, G. B.; Oakley, R. T.; Rose, E.; Schmittou, E. R.; Ibers, J. A. *J. Am. Chem. Soc.* **1981**, *103*, 516−533. (b) Hatada, M. H.; Tulinsky, A.; Chang, C. K. *J. Am. Chem. Soc.* **1980**, *102*, 7115−7116. (c) Guilard, R.; Lopez, M. A.; Tabard, A.; Richard, F.; Lecomte, C.; Brandes, S.; Hutchison, J. E.; Collman, J. P. *J. Am. Chem. Soc.* **1992**, *114*, 9877−9889. (d) Collman, J. P.; Hutchison, J. E.; Lopez, M. A.; Tabard, A.; Guilard, R.; Seok, W. K.; Ibers, J. A.; L'Her, M. *J. Am. Chem. Soc.* **1992**, *114*, 9869−9877. (e) Senge, M. O.; Gerzevske, K. R.; Graça, M.; Vicente, H.; Forsyth, T. P.; Smith, K. M. *Angew. Chem.* **1993**, *105*, 745−747. (f) Osuka, A.; Nakajima, S.; Nagata, T.; Maruyama, K.; Toriumi, H. *Angew. Chem.* **1991**, *103*, 579−580. (g) Fillers, J. P.; Ravichandran, K. G.; Abdalmuhdi, I.; Tulinsky, A.; Chang, C. K. *J. Am. Chem. Soc.* **1986**, *108*, 417−424. (h) Kim, K.; Collman, J. P.; Ibers, J. A. *J. Am. Chem. Soc.* **1988**, *110*, 4242−4246. (i) Karaman, R.; Blasko, A.; Almarsson, Ö.; Arasasingham, R.; Bruice, T. C. *J. Am. Chem. Soc.* **1992**, *114*, 4889−4898. (j) Cowan, J. A.; Sanders, J. K. M. *J. Chem. Soc., Perkin Trans. 1* **1987**, 2395−2402.

(5) (a) Setsune, J.; Yoshida, Z.-I.; Ogoshi, H. *J. Chem. Soc., Perkin Trans. 1* **1982**, 983−987. (b) Yang, C.-H.; Dzugan, S. J.; Goedken, V. L. *J. Chem. Soc., Chem. Commun.* **1986**, 1313−1315. (c) Collman, J. P.; Arnold, H. J. *Acc. Chem. Res.* **1993**, *26*, 586−592. (d) Collman, J. P.; Fish, H. T. *Inorg. Chem.* **1996**, *35*, 7922−7923. (e) Mizutani, T.; Uesaka, T.; Ogoshi, H. *Organometallics* **1995**, *14*, 341−346. (f) Jones, N. L.; Carroll, P. J.; Wayland, B. B. *Organometallics* **1986**, *5*, 33−37.

(6) (a) Mansuy, D.; Lecomte, J.-P.; Chottard, J.-C.; Bartoli, J. F. *Inorg. Chem.* **1981**, *20*, 3119−3121. (b) Summerville, D. A.; Cohen, I. A. *J. Am. Chem. Soc.* **1976**, *98*, 1747−1752. (c) Hoffmann, A. B.; Collins, D. M.; Day, V. W.; Fleischer, E. B.; Srivastava, T. S.; Hoard, J. L. *J. Am. Chem. Soc.* **1972**, *94*, 3620−3626. (d) Masuda, H.; Taga, T.; Osaki, K.; Sugimoto, H.; Mori, M.; Ogoshi, H. *J. Am. Chem. Soc.* **1981**, *103*, 2199−2203. (e) Wyslouch, A.; Latos-Grazynski, L.; Grzeszczuk, M.; Drabent, K.; Bartczak, T. *J. Chem. Soc., Chem. Commun.* **1988**, 1377−1378. (f) Scheidt, W. R.; Cheng, B.; Safo, M. K.; Cukiernik, F.; Marchon, J.-C.; Debrunner, P. G. *J. Am. Chem. Soc.* **1992**, *114*, 4420−4421. (g) Balch, A. L.; Latos-Grazynski, L.; Noll, B. C.; Olmstead, M. M.; Safari, N. *J. Am. Chem. Soc.* **1993**, *115*, 9056−9061. (h) Kobuke, Y.; Miyaji, H. *J. Am. Chem. Soc.* **1994**, *116*, 4111−4112. (i) Goff, H. M.; Scheidt, W. R. *Inorg. Chem.* **1984**, *23*, 315−321.

(7) (a) Buchler, J. W.; De Cian, A.; Fischer, J.; Kihn-Botulinski, M.; Paulus, H.; Weiss, R. *J. Am. Chem. Soc.* **1986**, *108*, 3652−3659. (b) Buchler, J. W.; Hüttermann, J.; Löffler, J. *Bull. Chem. Soc. Jpn.* **1988**, *61*, 71−77.

(8) Arasasingham, R. D.; Balch, A. L.; Olmstead, M. M.; Renner, M. W. *Inorg. Chem.* **1987**, *26*, 3562−3568.

(9) Setsune, J.; Takeda, H. *Tetrahedron Lett.* **1996**, *36*, 5903−5904.

(10) (a) Setsune, J.; Ito, S.; Takeda, H.; Ishimaru, Y.; Kitao, T.; Sato, M.; Ohya-Nishiguchi, H. *Organometallics* **1997**, *16*, 597−605. (b) Setsune, J.; Ikeda, M.; Ishimaru, Y.; Kitao, T. *Chem. Lett.* **1989**, 667−670.

(11) Setsune, J.; Saito, Y.; Ishimaru, Y.; Ikeda, M.; Kitao, T. *Bull. Chem. Soc. Jpn.* **1992**, *65*, 639−648.

(12) Setsune, J.; Ishimaru, Y.; Saito, Y.; Kitao, T. *Chem. Lett.* **1989**, 671−674.

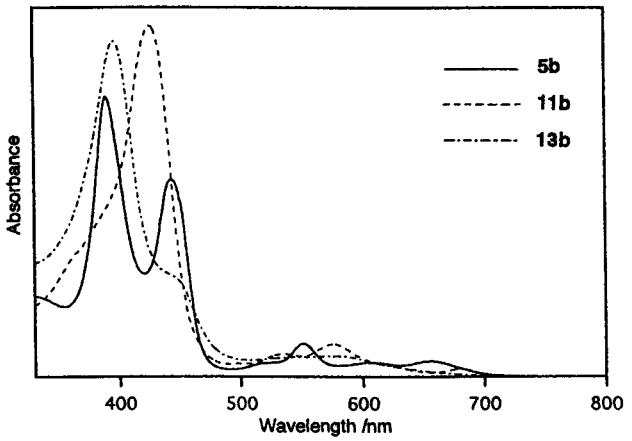


**Figure 1.** UV−vis spectra of (CH═CH-*Co*,*N*′)[(OEP)Co$^{III}$][(TPP)-$H_2$]$ClO_4$ (**5b**) (—), (CH═CH-*N*,*N*′)[(OEP)Co$^{II}$Cl][(TPP)H] (**11b**) (- - -), and (CH═CH-*N*,*N*′)[(OEP)H][(TPP)H] (**13b**) (- • -) in $CH_2Cl_2$.

way of vinylene-*Co*,*N*′-linked bis(porphyrin)s, because it is known that *σ*-(alkyl)Co$^{III}$ porphyrins are converted into *N*-alkylporphyrin Co$^{II}$ complexes.[13] Since porphyrin free bases as well as 2,6-lutidine are bulky amines, they are expected to attack the *π*-complexed acetylene ligand of cationic Co$^{III}$ porphyrins. This leads to vinylene-*Co*,*N*′-linked bis(porphyrin)s which contain a Co$^{III}$−C *σ*-bond.

When a mixture of (OEP[14])Co$^{III}$$(H_2O)_2ClO_4$ (**1a**) and a slight excess of (OEP)$H_2$ was allowed to react in dry $CH_2Cl_2$ under an atmosphere of purified acetylene gas, vinylene-*Co*,*N*′-linked bis(porphyrin) **5a** was obtained in a 91% yield after chromatographic purification on silica gel and recrystallization from $CH_2Cl_2$−hexanes. Other porphyrin free bases ((TPP)$H_2$, (TTP)$H_2$, N-Me(TTP)H[14] reacted analogously with **1a** and acetylene to afford **5b**−**d** in good yields (73−88%). (Perchlorato)Co$^{III}$ *meso*-tetraarylporphyrins gave lower yields of the vinylene-*Co*,*N*′-linked bis(porphyrin)s in comparison with **1a**. Thus, the reaction of (TPP)Co$^{III}$$(H_2O)_2ClO_4$ (**1b**) with (OEP)$H_2$ and $C_2H_2$ resulted in a 49% yield of (CH═CH-*Co*,*N*′)[(TPP)Co$^{III}$][(OEP)$H_2$]$ClO_4$ (**5e**). (CH═CH-*Co*,*N*′)[(TTP)Co$^{III}$][(TTP)$H_2$]$ClO_4$ (**5f**) was obtained in a 37% yield from (TTP)Co$^{III}$$(H_2O)_2ClO_4$ (**1c**), (TTP)$H_2$, and $C_2H_2$. UV−vis absorption bands characteristic of *σ*-(alkyl)Co$^{III}$ porphyrins and monoprotonated *N*-alkylporphyrins are observed for **5a**−**f**. For example, absorption bands at 391, 515, and 552 nm are ascribed to the Co$^{III}$(OEP) moiety and bands at 443, 609, and 655 nm to the *N*-vinyl(TPP)$H_2ClO_4$ moiety in the UV−vis spectrum of **5b** (Figure 1). The face-to-face bis(porphyrin) structures of **5a**−**f** are evidenced by a pair of upfield shifted doublets ($J_{trans}$ = ∼12 Hz) due to the Co−CH═ proton and the N−CH═ proton of the vinylene-*Co*,*N*′ linkage in the $^1$H NMR spectra. These vinylic proton chemical shifts (−3.62 ppm for Co−CH═ and −8.60 for ═CH−N) of (CH═CH-*Co*,*N*′)[(OEP)Co$^{III}$][(TPP)H] (**5b**′) are rationalized on the basis of the chemical shifts observed for monomeric porphyrins, *σ*-(*trans*-2-chlorovinyl)Co$^{III}$(OEP) (**6a**)[11] (−0.94 ppm for Co−CH═ and −1.63 for ═CH−Cl) and *N*-(*trans*-2-chlorovinyl)(TPP)H (**7**)[15] (2.30 ppm for Cl−CH═ and −1.45 for ═CH−N), assuming that the two porphyrins are linked by a *trans*-vinylene group with nearly parallel orientation of the two porphyrin planes and that the diamagnetic ring current effects from the two porphyrin rings on each vinylene proton are additive.

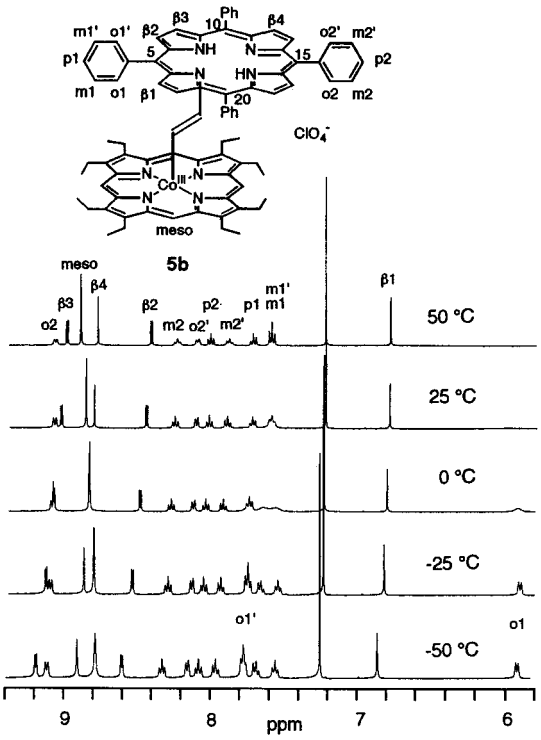


**Figure 2.** Variable-temperature $^1$H NMR spectra of the aromatic region of (CH═CH-*Co*,*N*′)[(OEP)Co$^{III}$][(TPP)$H_2$]$ClO_4$ (**5b**) in $CDCl_3$. The *ortho*-, *meta*-, and *para*-phenyl protons and *β*-pyrrole protons of TPP are denoted as "o", "m", "p", and "*β*", respectively. The OEP *meso* protons are denoted as "meso".

One of the four signals due to the *β*-pyrrole protons (*β*1−*β*4) is shifted to a higher magnetic field (6.82 ppm) than the others (9.06, 8.84, and 8.48 ppm) in the NMR spectrum of **5b** (Figure 2). This upfield-shifted signal is assigned to the *β*-pyrrole protons (*β*1) of the N-vinylated pyrrole which is in the highly shielding region due to the ring current effect of the OEP moiety. The complete assignment of the signals in the aromatic region of **5b** was made on the basis of the H−H COSY spectrum. The $^1$H-signals associated with the symmetry-related 10- and 15-*meso*-phenyl groups (o2, o2′, m2, m2′, p2) distant from the N$^{21}$-vinylated pyrrole appear below 7.8 ppm, since they are positioned in the deshielding region due to the ring current effect of the OEP moiety. These outer phenyl groups are not rotating rapidly on the NMR time scale at 25 °C, because five proton signals from each phenyl ring appear at discrete chemical shifts (9.11, 8.29, 8.14, 8.05, 7.93 ppm). On the other hand, the $^1$H-signals from the 5- and 20-*meso*-phenyl groups (o1, o1′, m1, m1′, p1) adjacent to the N$^{21}$-vinylated pyrrole are observed above 7.8 ppm, since these inner phenyl groups are in the shielding region of the OEP ring. The *ortho* proton signals (o1, o1′) are not observed at 25 °C because of the restricted rotation of these phenyl rings on the NMR time scale. They appear at 5.95 and 7.81 ppm at −25 °C. The appearance of a triplet signal due to the two *meta* protons (m1, m1′) at 25 °C is simply because of the coincidence of the chemical shifts of m1 and m1′. Thus, the 5- and 20-*meso*-aryl groups adjacent to the N$^{21}$-substituted pyrrole ring rotate faster than the 10- and 15-*meso*-aryl groups adjacent to the N-unsubstituted pyrrole rings. It has also been shown by Lavallee and co-workers that the rotational barrier of the 5- and 20-*meso*-aryl groups is

(13) (a) Dolphin, D.; Halko, D. J.; Johnson, E. *Inorg. Chem.* **1981**, *20*, 4348−4351. (b) Callot, H. J.; Metz, F.; Cromer, R. *Nouv. J. Chim.* **1984**, *8*, 759−763. (c) Callot, H. J.; Metz, F. *J. Chem. Soc., Chem. Commun.* **1982**, 947−948.

(14) Abbreviations: OEP (octaethylporphyrin dianion); TPP (*meso*-tetraphenylporphyrin dianion); TTP (*meso*-tetra-*p*-tolylporphyrin dianion); N-MeTTP (*N*-methyl-*meso*-tetra-*p*-tolylporphyrin anion).

(15) Setsune, J.; Ikeda, M.; Kishimoto, Y., Ishimaru, Y.; Fukuhara, K.; Kitao, T. *Organometallics* **1991**, *10*, 1099−1107.

different from that of the 10- and 15-*meso*-aryl groups in water-soluble $N^{21}$-methyl-*meso*-tetraarylporphyrins.[16] They tentatively assigned the $^1$H NMR signals that get broad at higher temperature to the 5- and 20-*meso*-aryl groups and suggested that the 5- and 20-*meso*-aryl groups are subjected to larger steric constraints than the 10- and 15-*meso*-aryl groups due to the tilting of the $N^{21}$-methylated pyrrole ring. Since the signal assignment is reliable in the case of vinylene-*Co,N′*-linked bis(porphyrin)s, we do not agree with their conclusion. We believe that the tilting of the N-substituted pyrrole ring relieves steric congestion between this pyrrole ring and the adjacent *meso*-aryl groups.

Whereas **5a**−**c** show a $C_{4v}$-symmetric pattern for the Co(OEP) resonances and a $C_s$-symmetric pattern for the N-substituted porphyrin resonances in their $^1$H NMR spectra, **5d** show a dissymmetric pattern for the N-Me(TTP) resonances and a $C_{4v}$-symmetric pattern for the OEP resonances. This implies that the *N*-methyl group and the N-vinyl group are positioned at the adjacent pyrrole nitrogens of TTP and that the rotation of the Co(OEP) moiety around the Co−C bond is very fast. The dialkylation at the $N^{21}$- and $N^{22}$-positions rather than the $N^{21}$- and $N^{23}$-positions is generally seen in the reaction of porphyrin free bases with alkylating agents.[17]

The reaction of a bis(porphyrin) free base, (CH═CH-*N,N′*)-[(TTP)H]$_2$ (**8**),[10,12] with 2.2 molar equiv of **1a** in dry $CH_2Cl_2$ at room temperature under $C_2H_2$ gas proceeded smoothly to provide a tris(porphyrin), (CH═CH-*Co,*$N^{22'}$)(CH═CH-$N^{21'}$,$N''$)-[(OEP)Co$^{III}$][(TTP)H]$_2$ClO$_4$ (**9**), and a tetrakis(porphyrin) (**10**), in 26 and 62% yields, respectively. The latter is a mixture of two regioisomers, (CH═CH-*Co,*$N^{22'}$)(CH═CH-$N^{21'}$,$N^{21''}$)-(CH═CH-$N^{22''}$,*Co*)[(OEP)Co$^{III}$]$_2$[(TTP)H]$_2$(ClO$_4$)$_2$ (anti-**10**) and (CH═CH-*Co,*$N^{22'}$)(CH═CH-$N^{21'}$,$N^{21''}$)(CH═CH-$N^{24''}$,*Co*)[(OEP)-Co$^{III}$]$_2$[(TTP)H]$_2$(ClO$_4$)$_2$ (syn-**10**), as depicted in Scheme 3. The FAB MS spectrum of **9** shows a molecular ion at *m*/*e* 2082 (Figure 3). An intense mass peak corresponding to a fragment ion with loss of a perchlorate ion was observed for **9** (*m*/*e* 1983) and **10** (*m*/*e* 2700). The stepwise elimination of an (OEP)Co unit and a $C_2H_2$ unit from a fragment ion at *m*/*e* 2600 ($M^+ + 1 - 2ClO_4$) in the case of **10** gives intense mass peaks at *m*/*e* 1983 (loss of (OEP)Co and $C_2H_2$), 1391 (loss of 2(OEP)Co and $C_2H_2$), and 1365 (loss of 2(OEP)Co and $2C_2H_2$). The tris(porphyrin) **9** could be generated as a main product in a 50% yield along with **10** in a 7% yield, if 1.4 molar equiv of **1a** was allowed to react with **8** in a diluted solution at 0 °C. The $^1$H NMR spectrum of **9** shows a 4H-singlet due to the OEP *meso* protons and eight 3H-singlets due to the methyl protons of the *p*-tolyl groups. This indicates that the N-vinylation in the middle layer porphyrin in the tris(porphyrin) **9** occurs at the $N^{21}$- and $N^{22}$-positions in a fashion similar to **5d**. A further N-vinylation at the terminal TTP moiety of **9** generates two regioisomers of **10** depending on whether the $N^{22}$- or $N^{24}$-position with respect to the original $N^{21}$-vinyl group is vinylated. These are the $C_i$-symmetric isomer (anti-**10**) and the $C_2$-symmetric isomer (syn-**10**). Although chromatographic separation of these isomers was unsuccessful, the $^1$H NMR spectrum of **10** shows two singlets due to the *meso* protons of the Co(OEP) moiety corresponding

**Scheme 3**

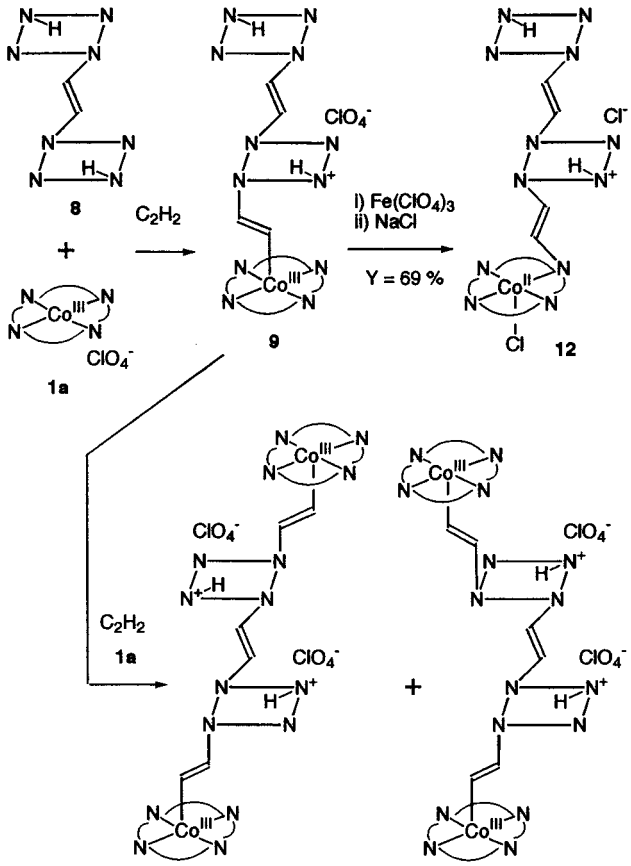


| ratio 1a / 8 | conc. of 8 (mM/L) | temp (°C) | Yield (%) 9 | 10 |
|---|---|---|---|---|
| 1.4 | 1.4 | 0 | 50 | 7 |
| 2.2 | 3.8 | 20 | 26 | 62 |

to anti-**10** and syn-**10** in the ratio of ca. 1:1. Two sets of proton signals due to the linking vinylene moiety appear at slightly different magnetic fields. That is, −4.75 and −4.84 ppm for the Co−CH═ proton, −11.28 and −11.21 ppm for the Co−C═CH−N proton, −6.19 and −6.28 ppm for the N−CH═CH−N protons, and −7.38 and −7.77 ppm for the NH proton.

It is reasonable that the chemical shifts of the Co−CH═ proton (from −3.62 to −4.38 and then to −4.75 (−4.84) ppm), the Co−C═CH−N proton (from −9.24 to −10.64 and then to −11.28 (−11.21) ppm), and the NH proton (from −4.75 to −6.03 and then to −7.38 (−7.77) ppm) of **5d**, **9**, and **10** move to higher fields with increase in the number of porphyrin layers.

**Vinylene-*N,N′*-Linked Multi(porphyrin)Co$^{II}$ complexes (11b,c,e, 12) and Free Bases (13a−c).** It has been pointed out that organoiron(III) and organocobalt(III) porphyrins rearrange to metal(II) N-substituted porphyrins upon one-electron oxidation and that the Co-to-N migration of an alkyl group is induced by one-electron oxidation at the Co site of *σ*-(alkyl)-Co$^{III}$ porphyrins.[13,18] Cyclic voltammetric analysis of the (vinylene-*Co,N′*)bis(porphyrin)s in $CH_2Cl_2$ (Table 1) showed two pseudoreversible redox couples at potentials similar to those

(16) Lavallee, D. K.; Xu, Z.; Pina, R. *J. Org. Chem.* **1993**, *58*, 6000−6008.

(17) (a) Broadhurst, M. J.; Grigg, R.; Shelton, G.; Johnson, A. W. *J. Chem. Soc., Chem. Commun.* **1970**, 231−232. (b) Grigg, R.; Sweeney, A.; Dearden, G. R.; Jackson, A. H.; Johnson, A. W. *J. Chem. Soc., Chem. Commun.* **1970**, 1273−1274. (c) Johnson, A. W.; Ward, D.; Batten, P.; Hamilton, A. L.; Schelton, G.; Elson, C. M. *J. Chem. Soc., Perkin Trans. 1* **1975**, 2076−2085. (d) Cavaleiro, J. A. S.; Condesso, M. F. P. N.; Jackson, A. H.; Neves, M. G. P. M. S.; Nagaraja Rao, K. R.; Sadashiva, B. K. *Tetrahedron Lett.* **1984**, *25*, 6047−6050.

(18) (a) Miyamoto, K.; Suenobu, T.; Itoh, S.; Fukuzumi, S. *Abstracts of the 42nd Symposium on Organometallic Chemistry*; Higashi-Hiroshima, Japan; 1995; p 166. (b) Lavallee, D. K. *The Chemistry and Biochemistry of N-Substituted Porphyrins*; VCH: Weinheim, Germany, 1987.

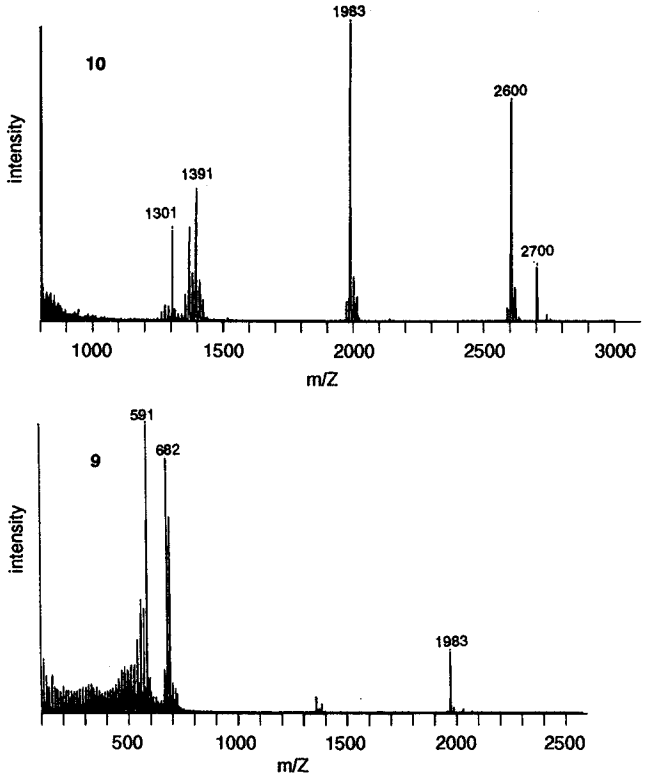


**Figure 3.** FAB MS spectra of the tris(porphyrin) (CH═CH-*Co*,*N*$^{22'}$)-(CH═CH-*N*$^{21'}$,*N*′)[(OEP)Co$^{III}$][(TTP)H]$_2$ClO$_4$ (**9**) (bottom) and the tetrakis(porphyrin) (**10**) (top). Matrix: *m*-nitrobenzyl alcohol.

**Table 1.** Electrochemical Data (V) for (Por)Co$^{III}$CH═CHR in $CH_2Cl_2$[a]

| no. | (Por)Co | R | $E_{pa}$ | $E_{pc}$ | $E_{1/2}$ |
|---|---|---|---|---|---|
| **6a** | (OEP)Co | Cl | 0.91 | 0.82 | 0.87 |
| | | | 1.26 | 1.17 | 1.22 |
| **5a** | (OEP)Co | (*N*-OEP)H$_2$ClO$_4$ | 0.98 | 0.89 | 0.94 |
| | | | 1.30 | 1.21 | 1.26 |
| **5c** | (OEP)Co | (*N*-TTP)H$_2$ClO$_4$ | 0.98 | 0.91 | 0.95 |
| | | | 1.29 | 1.25 | |
| **6c** | (TTP)Co | Cl | 1.08 | 0.97 | 1.03 |
| | | | 1.29 | 1.18 | 1.24 |
| **6e′** | (TTP)Co | (*N*-OEP)H$_2$ClO$_4$ | 1.05 | 0.98 | 1.02 |
| | | | 1.25 | 1.19 | 1.22 |

[a] Conditions: scan rate, 100 mV/s; supporting electrolyte, 0.1 M $Bu_4N^+ClO_4^-$; WE, glassy carbon; RE, Ag/AgCl; $E_{pa}$, anodic peak potentials; $E_{pc}$, cathodic peak potentials; $E_{1/2}$, half-wave potentials.

which correspond to the formation of Co$^{III}$ porphyrin $\pi$-cation radicals (or Co$^{IV}$ porphyrins) and Co$^{III}$ porphyrin $\pi$-dications (or Co$^{IV}$ porphyrin $\pi$-cation radicals) from $\sigma$-($\beta$-chlorovinyl)-Co$^{III}$ porphyrins (**6a**) and $\sigma$-(ClCH═CH)Co$^{III}$(TTP) (**6c**).[13a,18] A large increase in the anodic current beyond +1.5 V (vs Ag/AgCl) was observed only in the case of **5a**. This means that complex **5a** is decomposed at a less positive potential than the other *Co*,*N*′-linked bis(porphyrin)s examined here. In fact, **5a** lost a vinylene linkage and decomposed to its monomeric components by the treatment with Fe(ClO$_4$)$_3$, whereas the (vinylene-*Co*,*N*′)bis(porphyrin)s with at least one *meso*-tetraarylporphyrin moiety were successfully converted into the corresponding (vinylene-*N*,*N*′)bis(porphyrin)Co$^{II}$ complexes (**11b**,**c**,**e**) in 53−82% yields (Scheme 4). These complexes were isolated as combinations of a free-base form of one *N*-vinylporphyrin moiety and a high-spin ($S = {}^3/_2$) Co$^{II}$ complex with a chloride as an axial ligand in the other *N*-vinylporphyrin moiety. Their $^1$H NMR spectra show very sharp signals, and the signal assignment of (CH═CH-*N*,*N*′)[(OEP)Co$^{II}$Cl][(TPP)H]

**Scheme 4**

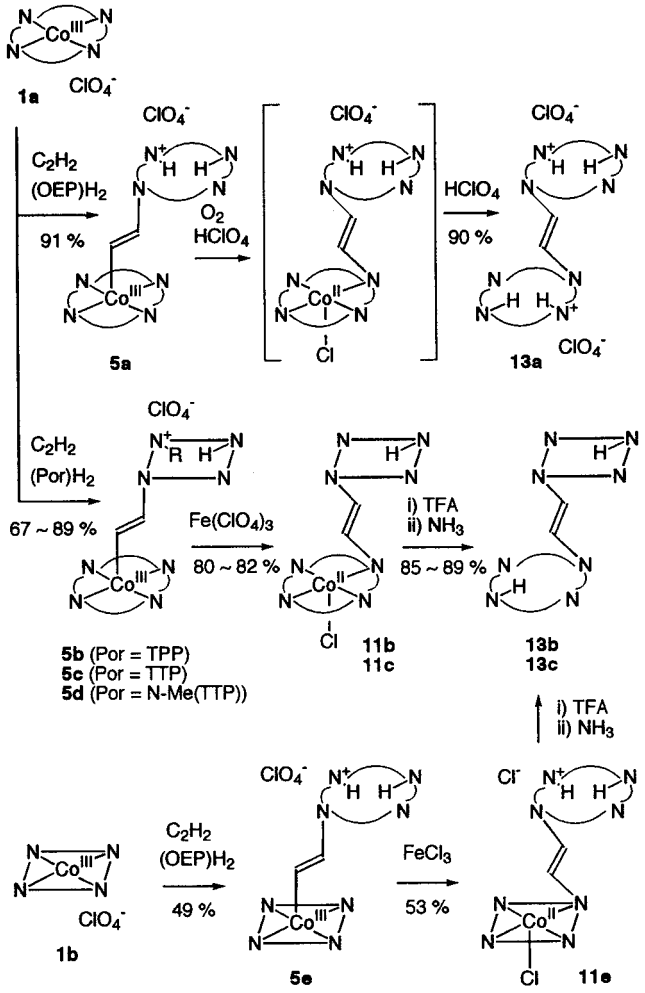


(**11b**) was made by the H−H COSY spectrum. The chemical shifts and the splitting patterns for the $^1$H-signals due to the OEP periphery are typical of N-substituted (OEP)Co$^{II}$ complexes such as N-($CH_2CH_2CH_2I$)(OEP)Co$^{II}$Cl.[9,10,19] That is, eight diastereotopic $CH_2$ signals (36.3, 26.9, 23.3, 20.4, 19.2, 19.0, 14.0, 13.8 ppm), four 6H-methyl signals (9.9, 8.2, 2.7, 0.7 ppm), and two 2H-*meso* signals (13.9, −10.8 ppm) are indicative of the $C_s$-symmetric OEP structure. The two protons of the vinylene-*N*,*N*′ linkage appear at −106 and −78.2 ppm, which are associated with the Co$^{II}$(OEP) side and the TPP side, respectively, as judged by their line widths, 900 and 90 Hz, respectively. A signal at −20.7 ppm is assigned to the NH proton of the TPP core, because it is exchangeable with $D_2O$. One set of spin-coupled sharp signals (two doublets at 6.35 and 4.80 ppm; three triplets at 7.50, 7.17, and 6.40 ppm) are associated with the 10- and 15-*meso*-phenyl protons of the N$^{21}$-substituted TPP moiety of **11b**, because these chemical shifts are not subjected to large paramagnetic shifts from Co. Another set of phenyl proton signals are observed as broad signals at the chemical shifts (9.9 and 4.7 for *ortho*; 14.7 and 7.7 for *meta*; 10.0 for *para*), which are shifted by the paramagnetic effect of Co. Thus, these phenyl groups are at the 5- and 20-*meso* positions of TPP close to Co.

The complex **5e** with a $\sigma$-(vinyl)Co$^{III}$(TPP) moiety was similarly converted into the corresponding (vinylene-*N*,*N*′)bis-(porphyrin), (CH═CH-*N*,*N*′)[(TPP)Co$^{II}$Cl][(OEP)H$_2$]Cl (**11e**),

(19) Latos-Grazynski, L. *Inorg. Chem.* **1985**, *24*, 1104−1105.

with a $Co^{II}$ ion in the TPP core. The complex **11e** was isolated as a monoprotonated form due to a more basic nature of the N-substituted OEP pyrrole nitrogens than the corresponding TPP pyrrole nitrogens. The signals due to the TPP periphery of **11e** are subjected to large paramagnetic shifts by the presence of a high-spin $Co^{II}$ ion in the TPP core, whereas the signals due to the OEP periphery appear in a diamagnetic chemical shift range. The isotropic shifts observed for the $\beta$-pyrrole protons and *N*-vinyl protons of **11e** are similar in size to those of *N*-(CH═CHCl)(TPP)$Co^{II}$(SCN).[10] The mono-$Co^{II}$ complexes, **11b**,**c**,**e**, were readily demetalated by $CF_3CO_2H$ to provide bis(porphyrin) free bases, **13b**,**c**, after workup with aqueous ammonia. The UV−vis spectra of **11b** and **13b** are shown in Figure 1. The $Co^{II}$ complexes, **11b** and **11e**, gave the same bis(porphyrin), (CH═CH-*N*,*N*′)[(OEP)H][(TPP)H] (**13b**), which shows a pair of doublets ($J_{trans}$ = 12.3 Hz) due to the vinylene protons at $\delta$ −5.83 and −6.45. Whereas oxidation of the complex **5a** with ferric ion led to the decomposition of the bis(porphyrin) framework as noted before, the treatment of a $CH_2Cl_2$ solution of **5a** with aqueous 60% $HClO_4$ under aerobic conditions successfully caused Co-to-N migration of the vinylene linkage to give (CH═CH-*N*,*N*′)[(OEP)$H_2$]$_2$($ClO_4$)$_2$ (**13a**) as a diprotonated form in a 90% yield. The *N*,*N*′-vinylene protons of **13a** are chemically equivalent and therefore appear as a 2H-singlet at −8.40 ppm in the $^1$H NMR spectrum. This migration of a $\sigma$-vinyl group from Co to nitrogen under strongly acidic conditions is considered to be induced by air oxidation, as had been reported in the case of simple organocobalt(III) porphyrins by Callot et al.[13c] The strongly acidic conditions prevent the nucleophilic attack of the porphyrin nitrogen on the linking vinylene carbon which should be responsible for the decomposition of the bis(octaethylporphyrin) structure.

The *Co*,*N*′-linked tris(porphyrin) **9** was analogously oxidized to give an N-substituted tris(porphyrin)$Co^{II}$ complex, (CH═CH-$N_{OEP}$,$N^{22'}$)(CH═CH-$N^{21'}$,$N''$)[(OEP)$Co^{II}$Cl][(TTP)H]$_2$Cl (**12**), in a 69% yield. The MALDI MS spectrum of **12** shows the heaviest ion peak at *m*/*e* 2022. This mass number corresponds to a fragment ion with loss of one counteranion from the parent ion. The dissymmetric molecular structure of **12** is indicated by the appearance of four *meso*-protons of the OEP periphery and eight methyl groups of the bis(TTP) peripheral *p*-tolyl groups at different chemical shifts (13.0, 10.2, −11.0, −11.3 ppm for *meso*-H; 6.31, 3.84, 3.18, 2.54, 2.54, 2.12, 1.96, 1.93 ppm for methyl) in the $^1$H NMR spectrum.

**Homo- and Heterobimetallic Complexes of Vinylene-*N*,*N*′-Linked Bis(porphyrin)s (14a−c, 15a,b).** The mixed bis(porphyrin) free base **13b** was metalated with $Co^{II}(OAc)_2$, $Cu^{II}Cl_2$, and $Zn^{II}(OAc)_2$ in methanol followed by axial ligand exchange with an aqueous NaCl solution to give homobinuclear bis(porphyrin) complexes (CH═CH-*N*,*N*′)[(OEP)$M^{II}$Cl][(TPP)-$M^{II}$Cl] (**14a** (M = Co), **14b** (M = Cu), **14c** (M = Zn)), in 59, 75, and 82% yields, respectively (Scheme 5). The bis-$Co^{II}$ complex **14a** shows sharp paramagnetic $^1$H NMR signals, while the $^1$H NMR spectrum of the bis-$Cu^{II}$ complex **14b** is too broad to make signal assignments. The $^1$H chemical shifts of both the OEP periphery and the TPP periphery in the bis-$Co^{II}$ complex **14a** are typical of N-substituted porphyrin $Co^{II}$ complexes, and the very large upfield chemical shift (−182 ppm) for the *N*,*N*′-vinylene protons is reasonable since the isotropic shifts of the two high-spin $Co^{II}$ centers are additive.[10a]

The mono-$Co^{II}$ complex of (vinylene-*N*,*N*′)bis(porphyrin) **11b** was readily metalated with $CuCl_2$ and $ZnCl_2$ to give heterobinuclear bis(porphyrin)s, (CH═CH-*N*,*N*′)[(OEP)$Co^{II}$Cl][(TPP)-$M^{II}$Cl] (**15a** (M = Cu), **15b** (M = Zn)), in 75 and 88% yields,

**Scheme 5**

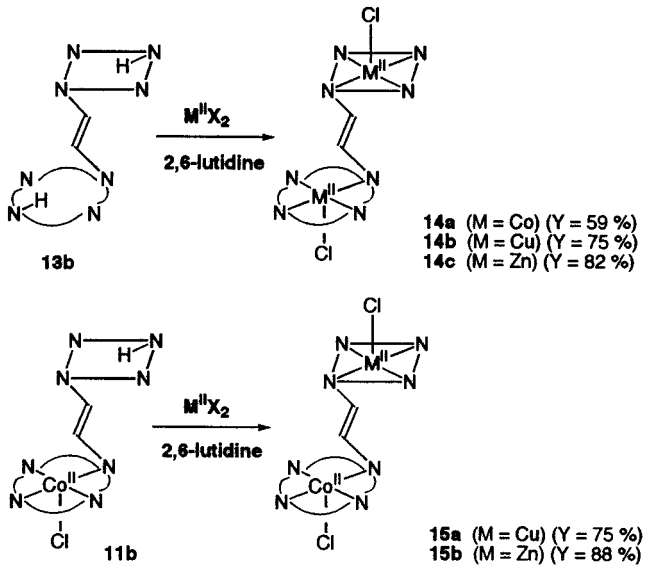


respectively. The CoZn complex **15b** shows a well-resolved paramagnetic $^1$H NMR spectrum which is nearly identical to that of **11b** except that a NH proton signal observed at −20.7 ppm for **11b** disappear. A $Cu^{II}$ ion in the TPP site of **15a** does not have a remarkable effect on the chemical shifts of the $^1$H NMR resonances due to the OEP protons, although it has great influence on the line widths. As shown in Figure 4, the four methyl signals (c1−4) due to the OEP periphery of **15a** appear at substantially the same magnetic fields (9.9, 7.8, 0.3, −1.0 ppm) as those of **15b** (9.6, 7.8, 0.4, −1.1 ppm). Whereas all the latter signals are very sharp, one of the former signals at −1.0 ppm (c4) is too broad to give cross-peaks in the H−H COSY spectrum. The $CH_2$ protons next to this $CH_3$ group (c4) are assigned to two broad signals (b4 and b4′) at $\delta$ 19.8 and 15.2 on the basis of the chemical shift data of **15b**. This set of three broad signals (b4, b4′, and c4) are associated with the ethyl groups at the N-substituted pyrrole ring of the OEP nucleus because they are spatially close to the Cu ion in the TPP core. The chemical shift differences between **15a** and **15b** are within 0.3 ppm for all the OEP protons and within 0.4 ppm for the *meta*- and *para*-phenyl protons of the TPP moiety. The signals due to the *ortho*-phenyl protons of **15a**, however, are not only shifted by up to 2.3 ppm but also undergo broadening with respect to the corresponding signals of **15b**. This is because of the proximity of the *ortho*-phenyl protons to the $Cu^{II}$ ion.

A $Cu^{II}$ ion in the TPP site of **15a** causes serious effects on the signals due to the $\beta$-pyrrole protons and the *N*,*N*′-vinylene protons. The isotropic shifts by $Cu^{II}$ to the $\beta$-pyrrole protons are remarkable in comparison with the chemical shifts (5.4−4.5 ppm) of those in the complex **15b**. A very broad signal centered at 43 ppm ($\beta$2−4) with a line width of ca. 2200 Hz may be associated with the $\beta$-pyrrole protons of the N-unsubstituted pyrrole rings. This chemical shift is analogous to the reported value (41 ppm with a line width of 1150 Hz) for the $\beta$-pyrrole deuteron resonance in (TPP-$d_8$)$Cu^{II}$.[20] It is known that a $^1$H NMR signal is by 42 times wider than a $^2$H NMR signal in the special case where the NMR line width is directly proportional to the square of the gyromagnetic ratio of the nucleus.[21] The observed line width of the $^1$H signal at 43 ppm in the present case is well reduced probably because the

(20) Godziela, G. M.; Goff, H. M. *J. Am. Chem. Soc.* **1986**, *108*, 2237−2243.

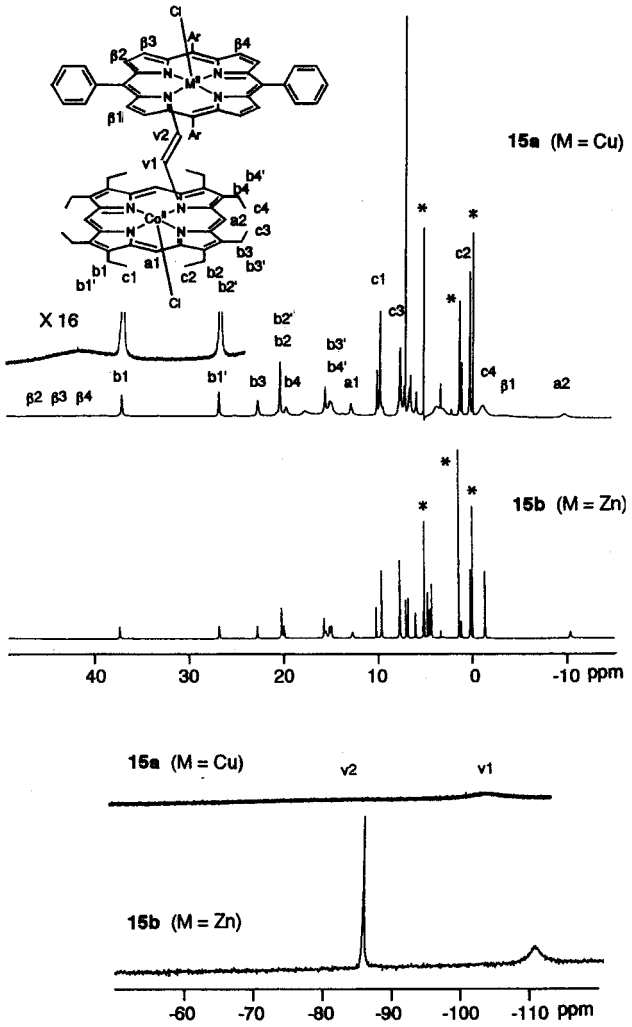


**Figure 4.** Paramagnetic $^1$H NMR spectra of (CH═CH-*N*,*N*′)[(OEP-)Co$^{II}$Cl][(TPP)Cu$^{II}$Cl] (**15a**) and (CH═CH-*N*,*N*′)[(OEP)Co$^{II}$Cl][(TPP)-Zn$^{II}$Cl] (**15b**) in $CDCl_3$. The *meso*-H, $CH_2$, and $CH_3$ signals of OEP are denoted as "a", "b", and "c", respectively. The $\beta$-pyrrole protons of TPP and the vinylene protons are denoted as "$\beta$" and "v". The signals of $CHCl_3$, $CH_2Cl_2$, $H_2O$, and TMS are indicated by asterisks.

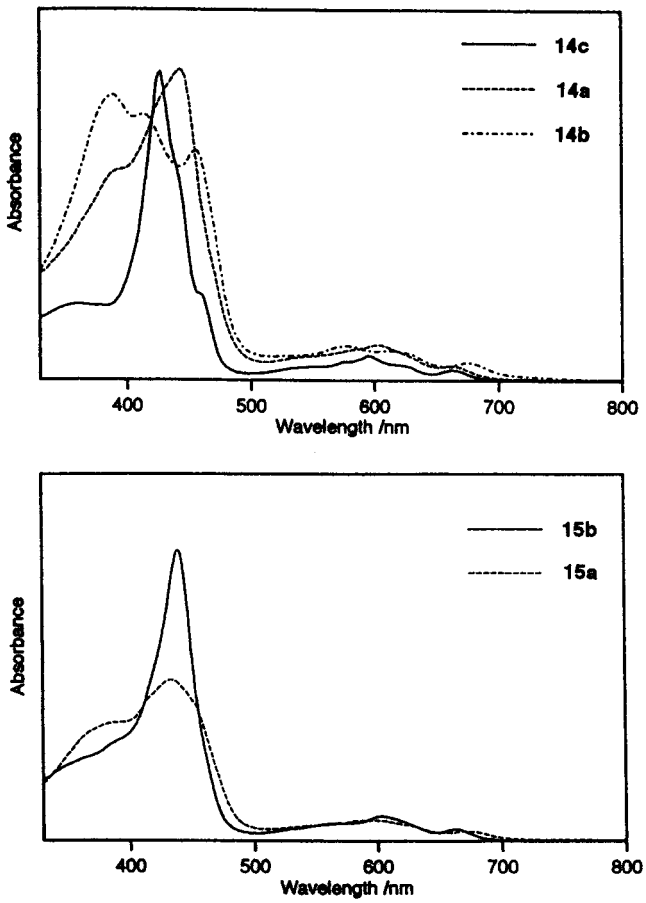


**Figure 5.** UV−vis spectra of the homobinuclear complexes (top), **14a** (CoCo) (- - -), **14b** (CuCu) (- • -), and **14c** (ZnZn) (—), and the heterobinuclear complexes (bottom), **15a** (CoCu) (- - -) and **15b** (CoZn) (—), in $CH_2Cl_2$.

relaxation of a Cu$^{II}$ electron spin is promoted by an intramolecular Co$^{II}$ electron spin. The influence of the paramagnetism of Cu on the $\beta$-pyrrole protons of the N-substituted pyrrole ring seems to be smaller than on those of the N-unsubstituted pyrrole rings, because of a weaker Cu−N bonding in the case of the N-substituted pyrrole nitrogen. Therefore, a relatively sharp signal at −3.5 ppm ($\beta$1) with a line width of ca. 200 Hz may be associated with the $\beta$-pyrrole protons of the N-substituted pyrrole ring. A very broad resonance centered at ca. −80 ppm (v2) with a line width of ca. 4000 Hz is assigned to the *N*,*N*′-vinylene proton on the Cu side, because the proximity of this proton to Cu$^{II}$ is responsible for its extremely large line broadening. A less broad resonance at −106 ppm (v1) is associated with the *N*,*N*′-vinylene proton on the Co side. The line width at a half-height of this signal increases from 350 Hz in **15b** to 2200 Hz in **15a**. These chemical shifts due to the *N*,*N*′-vinylene protons of **15a** are similar to those of **15b** (−85 and −110 ppm). Since the $S = {}^1/_2$ spin resides in the $d_{x^2-y^2}$ orbital of Cu$^{II}$, it is transmitted through the Cu−N $\sigma$-bonds to the $\beta$-pyrrole protons via four bonds between Cu and H. The spin transmission is much more effective to the $\beta$-pyrrole protons than to the *N*,*N*′-vinylene protons despite the greater number of bonds intervening between Cu and the $\beta$-pyrrole H, because the path (4 $\sigma$-bonds) through which the spin density is transmitted to the $\beta$-pyrrole H is within the same plane as the $d_{x^2-y^2}$ orbital of Cu$^{II}$.

The UV−vis spectra of the homobinuclear complexes, **14a**−**c**, and the heterobinuclear complexes, **15a**,**b**, are superpositions of rhodo type spectral patterns characteristic of N-substituted OEP metal complexes and N-substituted TPP metal complexes (Figure 5).

The X-ray crystal structure with an atom-numbering scheme and the crystallographic data for **15b** are shown in Figure 6 and Table 2. Two porphyrin planes in the complex **15b** are in a parallel orientation to avoid steric interactions, as is seen from the dihedral angle (5.8°) between two planes, PL1 and PL2, which are defined by three unsubstituted pyrrole nitrogens of OEP (N2, N3, N4) and TPP (N6, N7, N8), respectively. Although two peripheral ethyl groups of OEP at C3 (N1-pyrrole ring) and C12 (N3-pyrrole ring) are disordered, the positions of the remaining six ethyl groups are determined with certainty. These ethyl groups are directed toward the TPP plane probably due to the requirement of crystal packing, with only one exception at C7 (N2-pyrrole ring). The region of the closest intramolecular contact of the OEP nucleus and the TPP nucleus is between the N2-pyrrole ring of OEP and the N6-pyrrole ring of TPP. The C45 atom of the N6-pyrrole ring is 3.677(7) and 3.565(7) Å distant from the C6 and C7 atoms, respectively, of the N2-pyrrole ring. Therefore, the methylene carbon C25

(21) Swift, T. J. *NMR of Paramagnetic Molecules*; La Mar, G. N., Horrocks, W. DeW., Holm, R. H., Eds.; Academic Press: New York, 1973; pp 53−83.

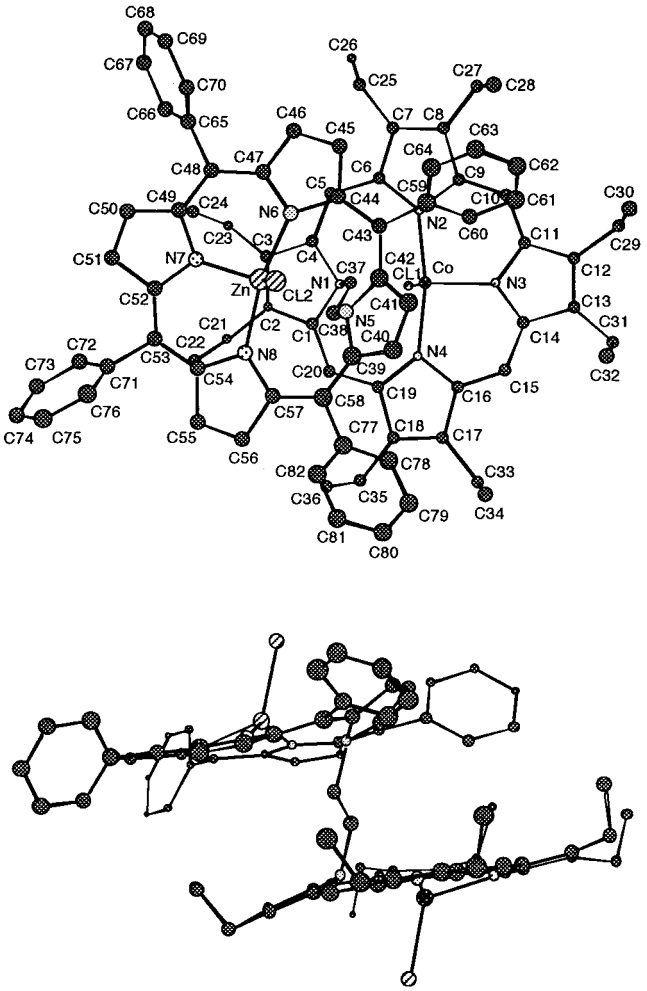


**Figure 6.** X-ray structure of (CH═CH-*N*,*N*′)[(OEP)Co$^{II}$Cl][(TPP)Zn$^{II}$-Cl] (**15b**) with a numbering scheme (top) and a side view of the face-to-face structure of **15b** (bottom). Two ethyl groups at the $\beta$-pyrrole carbons (C2 and C13) are disordered, and only the major conformations are shown. The $CH_2Cl_2$ molecule is omitted for clarity.

**Table 2.** Crystallographic and Structure Refinement Data for **15b**

| | |
|---|---|
| formula | $C_{82}H_{74}N_8CoZnCl_2 \cdot CH_2Cl_2$ |
| fw | 1451.7 |
| temperature | 24.0 °C |
| radiation | Mo K$\alpha$ ($\lambda$ = 0.710 69 Å) |
| cryst system | triclinic |
| space group | $P\bar{1}$ |
| unit cell dimens | $a$ = 14.806(4) Å, $\alpha$ = 97.69(3)° |
| | $b$ = 18.703(10) Å, $\beta$ = 99.57(2)° |
| | $c$ = 13.796(3) Å, $\gamma$ = 96.74(3)° |
| $V$, $Z$ | 3694(2) Å$^3$, 2 |
| $d$(calc) | 1.305 g/cm$^3$ |
| $F_{000}$ | 1510 |
| $\mu$(Mo K$\alpha$) | 7.44 cm$^{-1}$ |
| cryst size | 0.15 × 0.40 × 0.40 mm |
| $2\theta_{max}$ | 50.0° |
| no. of reflcns measd | total: 13 562 |
| | unique: 13 010 ($R_{int}$ = 0.015) |
| structure solution | direct methods (SIR92) |
| refinement | full-matrix least squares |
| GOF | 2.72 |
| no. of observns ($I > 3.0\sigma(I)$) | 8239 |
| no. of variables | 906 |
| residuals: $R = \sum(\|F_o\| - \|F_c\|)/\sum F_o$; $R_w = [\sum w(\|F_o\| - \|F_c\|)^2/\sum wF_o^2]^{1/2}$ | 0.059; 0.042 |

adjacent to C7 is also very close to C45 (3.547(8) Å) and C46 (3.634(8) Å) of the N6-pyrrole ring of TPP. This explains why the ethyl group at C7 is pointed away from the TPP plane.

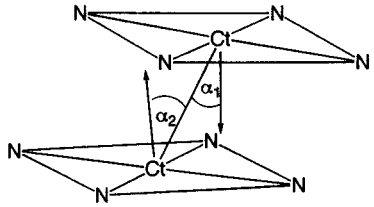


**Figure 7.** Structural parameters in the bis(porphyrin) systems.

**Table 3.** Inter-Ring Separations ($S_r$) and Slippages ($S_p$) in Bis(porphyrin)s Including **15b**[a]

| | Ct−Ct (Å)[b] | tilt (deg)[c] | α (deg)[d] | $S_r$ (Å)[e] | $S_p$ (Å)[f] | ref |
|---|---|---|---|---|---|---|
| (DPE)$Cu_2$ | | | | 3.36 | | 4e |
| (DPP)$H_2$ | | | | 3.43 | | 4f |
| (DPB)$Cu_2$ | 3.807 | 4.4 | 25.0 | 3.45 | 1.63 | 4g |
| (DPB)CoAl(OEt) | 4.08 | 7.4 | 29.8 | 3.54 | 2.03 | 4c |
| (DPA)$Ni_2$ | | 4.566 | 31.7 | 3.88 | 2.40 | 4g |
| (FTF4)$Co_2$ | 3.417 | 0.24 | 2.2 | 3.54 | 0.13 | 4h |
| (FTF6)$Cu_2$ | 6.33 | | 51.4 | 3.87 | 4.95 | 4a |
| (DP7)$Cu_2$ | | 5.22 | 46.4 | 3.52 | 3.80 | 4b |
| (O-*Co*,*N*)(DP) | | 2.2 | | 3.34 | | 8 |
| **15b** | 5.47 | 6.2 | 39.0 | 4.39[g] | 3.44 | this work |

[a] Abbreviations. DPE, *meso*-1,2-ethene-linked diporphyrin; DPP, *meso*-1,2-phenylene-linked diporphyrin; DPB, *meso*-1,8-biphenylene-linked diporphyrin; DPA, *meso*-1,8-anthracene-linked diporphyrin; FTF4, face-to-face diporphyrin with two four-atom amide spacers; FTF6, face-to-face diporphyrin with two six-atom amide spacers; DP7, diporphyrin with two seven-atom spacers; (O-*Co*,*N*)(DP), diporphyrin linked by a Co−O−N linkage. [b] Distances between the centers of the four nitrogens of porphyrins. [c] Dihedral angles between two porphyrin planes (24-atom least-squares plane). [d] $\alpha = (\alpha_1 + \alpha_2)/2$ ($\alpha_1$ and $\alpha_2$ are defined in the Figure 7). [e] $S_r = (Ct-Ct') \cos(\alpha)$. [f] $S_p = (Ct-Ct') \sin(\alpha)$. [g] Corrected for the deviations of the four-nitrogen centers (Ct) from the 24-atom least-squares planes.

The distance (Ct−Ct′) between the centers of four nitrogens of OEP and TPP is 5.47 Å. The angles ($\alpha_1$ and $\alpha_2$) between a Ct−Ct′ vector and the unit vectors normal to the least-squares planes of the 24-atom cores of OEP (PL11) and TPP (PL12) are 40.0 and 38.0°, respectively (Figure 7). The slip angle ($\alpha$) defined as an average of these two angles ($\alpha_1$ and $\alpha_2$) is 39.0°. The inter-ring separation ($S_r$ = (Ct−Ct′) cos($\alpha$)) is calculated to be 4.39 Å taking into account the inward deviations of the four-nitrogen centers (Ct) of OEP and TPP from the 24-atom least-squares planes of OEP and TPP (0.03 and 0.11 Å), respectively. The slippage ($S_p$ = (Ct−Ct′) sin($\alpha$)) is calculated as 3.44 Å. The $S_r$ value of **15b** is noticeably larger than the distance of a van der Waals contact between two porphyrin rings (ca. 3.4 Å). This separation is unique in view of the fact that the van der Waals interaction leads to a small range of inter-ring separations approaching van der Waals contacts for a diversity of bridging groups between porphyrin rings (Table 3).[4]

As indicated by the torsion angles (Co−N1−C37−C38 and Zn−N5−C38−C37) in Table 4, the pseudo $C_s$-symmetric plane in each N-substituted porphyrin unit (the Co−N1−C37 plane and the Zn−N5−C38 plane) is rotated by 128.6 and 108.3°, respectively, with respect to the *N*,*N*′-vinylene plane. This results in a 20.3° twisting of the TPP plane with respect to the OEP plane.

The structural features of the coordination spheres of Co$^{II}$ and Zn$^{II}$ of **15b** are similar to those of the corresponding (*N*-alkylporphyrin)metal(II) complexes previously reported, i.e., *N*-($CH_2CO_2Et$)(OEP)Co$^{II}$Cl (**16**)[23] and *N*-Me(TPP)Zn$^{II}$Cl (**17**),[24] respectively (Figure 8 and Table 4). One of the most unusual

(22) Evans D. F. *J. Chem. Soc.* **1959**, 2003.

**Table 4.** Selected Bond Lengths (Å) and Angles (deg) with Standard Deviations in Metal(II) *N*-Alkylporphyrin Complexes[a] **15b**, **16**,[b] and **17**[c]

| | | **15b** | | |
|---|---|---|---|---|
| | **16** (M = Co) | M = Co | M = Zn | **17** (M = Zn) |
| M−M | | 6.646(1) | | |
| M−Cl | 2.271(2) | 2.276(2) | 2.234(2) | 2.232(3) |
| M−N1(5) | 2.455(5) | 2.414(4) | 2.559(4) | 2.530(7) |
| M−N2(6) | 2.063(5) | 2.062(4) | 2.086(4) | 2.089(6) |
| M−N3(7) | 1.992(5) | 2.004(4) | 2.016(4) | 2.018(9) |
| M−N4(8) | 2.072(5) | 2.059(4) | 2.098(4) | 2.081(9) |
| N1(5)−C1(39) | 1.427(8) | 1.419(5) | 1.436(6) | 1.40(1) |
| N1(5)−C4(42) | 1.411(8) | 1.421(6) | 1.412(5) | 1.40(1) |
| C1(39)−C2(40) | 1.404(9) | 1.405(6) | 1.407(6) | 1.41(2) |
| C4(42)−C3(41) | 1.409(9) | 1.424(6) | 1.404(6) | 1.43(2) |
| C2(40)−C3(41) | 1.386(8) | 1.379(7) | 1.358(7) | 1.35(1) |
| M−N1(5)−C37(38) | 95.3(2) | 91.9(3) | 90.9(3) | 94.1(5) |
| Cl−M−N1(5) | 91.2(1) | 93.8(1) | 92.4(1) | 94.6(2) |
| Cl−M−N2(6) | 102.7(1) | 104.9(1) | 103.1(1) | 107.4(2) |
| Cl−M−N3(7) | 119.0(1) | 118.7(1) | 124.1(1) | 120.8(2) |
| Cl−M−N4(8) | 109.1(1) | 103.7(1) | 105.8(1) | 105.6(2) |
| Co−N1−C37−C38 | | 128.6(5) | | |
| Zn−N5−C38−C37 | | 108.3(5) | | |
| N1(5)−ring cant | 44.1 | 25.4 | 37.4 | 38.5 |
| N2(6)−ring cant | −8.3 | −6.6 | −6.7 | −11.6 |
| N3(7)−ring cant | −10.8 | −11.8 | −1.6 | −5.3 |
| N4(8)−ring cant | −12.2 | −7.8 | −11.2 | −12.3 |
| PL1-PL2 | | 174.2 | | |
| out of 3N-plane displacement of M | 0.61 | 0.56 | 0.60 | 0.65 |

[a] Atom numberings are according to Figures 6 and 8. [b] Taken from ref 23. [c] Taken from ref 24.

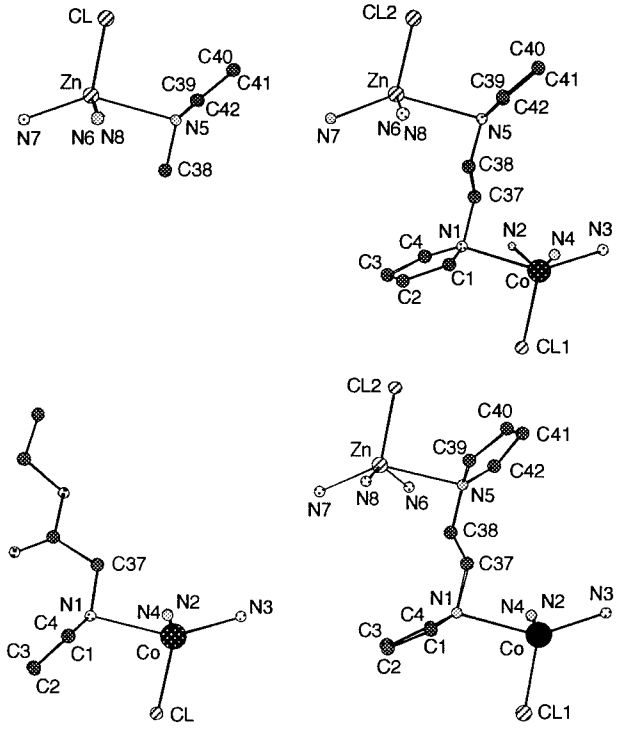


**Figure 8.** Comparison of the Co and Zn coordination spheres of **15b** (right) with those of *N*-alkyl(OEP)Co$^{II}$Cl (**16**) (bottom left) and *N*-alkyl-(TPP)Zn$^{II}$Cl (**17**) (top left), respectively.

features in the structure of **15b** is a small cant of the N1-pyrrole ring (PL3; the least-squares plane defined by N1, C1, C2, C3, and C4) with respect to the OEP plane (PL1). This dihedral angle (25.4°) is much smaller than the corresponding angles of (*N*-alkylporphyrin)metal(II) complexes including **16** (44.1°). The angle of the N1−C37 bond with respect to the N1-pyrrole ring, however, is 50.2° for **15b** in contrast to 37.0° for **16**. As a result of these, the direction of the N-substituted group with respect to the porphyrin plane is almost unchanged between the two complexes, **15b** and **16**. This is seen from the Co−N1−C37 angle of **15b** (91.9°) and **16** (95.3°). On the other hand, the face-to-face structure of **15b** does not cause a special structural change in the coordination sphere of Zn in comparison with **17**.

## Conclusion

We have shown in this paper that bis(porphyrin)s with a vinylene-*Co*,*N*′ or a vinylene-*N*,*N*′ linkage have been prepared via novel organometallic reactions of Co porphyrins with acetylene. The tris- and tetrakis(porphyrin)s are also prepared by the iterative use of this procedure. The $^1$H NMR spectroscopic investigation and single-crystal X-ray analysis have revealed characteristics in the molecular structure of the mixed-metal complexes of vinylene-*N*,*N*′-linked bis(porphyrin)s with a combination of different porphyrins. The stability of the compounds including their metal complexes, the solubility of the higher order multi(porphyrin) derivatives, the unique molecular structure based on the N-substitution, and the ease with which these multi(porphyrin)s are prepared provide an interesting family of the face-to-face porphyrin frameworks for further study of supramolecular chemistry.

## Experimental Section

UV−visible spectra were measured on a Shimadzu UV-2200 spectrophotometer. $^1$H NMR (250 MHz) spectra were recorded on a Bruker AM-250 spectrometer in $CDCl_3$. $^1$H-chemical shifts are referenced with respect to tetramethylsilane (0 ppm) as an internal standard. FAB MS and MALDI MS spectra were measured at the acceleration voltages of 8 and 5 kV on a Shimadzu/Kratos Concept IS mass spectrometer and a Shimadzu Kompact MALDI IV tDE spectrometer using *m*-nitrobenzyl alcohol and dithranol as matrixes, respectively. Cyclic voltammetry was carried out with a combination of a Hokuto Denko HB104 function generator and a HA301 potentiostat on a glassy carbon electrode using an Ag/AgCl couple as a reference electrode and tetrabutylammonium perchlorate (TBAP) as a supporting electrolyte in $CH_2Cl_2$ (scan rate 100 mV/s; scan range −0.1 to +1.8 V). Elemental analyses of C, H, and N were made with a Yanaco CHN corder. Kieselgel 60$F_{254}$ silica gel plates (Merck), Wakogel C-300 silica gel (Wako Junyaku), and aluminum oxide 90 (activity II-III; Merck) were used for TLC and column chromatography. Acetylene gas (99.99%) was generously supplied from Nichigo Acetylene Co. Ltd., Osaka, Japan. $CH_2Cl_2$ was distilled from $CaH_2$ and stored over 4A molecular sieves. (OEP)Co$^{III}$(H$_2$O)$_2$ClO$_4$ (**1a**), (TPP)Co$^{III}$(H$_2$O)$_2$ClO$_4$ (**1b**), and (TTP)Co$^{III}$(H$_2$O)$_2$ClO$_4$ (**1c**) were prepared according to the literature methods.[25]

**Vinylene-*Co*,*N*′-bis(porphyrin)s (5a−f). General Procedure.** A flask charged with (OEP)Co$^{III}$(H$_2$O)$_2$ClO$_4$ (**1a**) (0.10 mmol), a slight excess amount (0.11−0.14 mmol) of a free-base porphyrin [(OEP)H$_2$, (TPP)H$_2$, (TTP)H$_2$, *N*-Me(TTP)H], and $CH_2Cl_2$ (30 mL) was filled with an atmospheric pressure of acetylene gas. The whole mixture was stirred vigorously at 0−5 °C for 2 h. When bis(aquo)(*meso*-tetraarylporphyrinato)cobalt(III) perchlorates **1b**,**c** are used instead of **1a**, acetylene gas was introduced into a $CH_2Cl_2$ solution of two reactants, because a vigorous reaction occurs even in the solid state. $CH_2Cl_2$ was evaporated, and the residue was extracted with methanol to remove

(23) Goldberg, D. E.; Thomas, K. M. *J. Am. Chem. Soc.* **1976**, *98*, 913−919.
(24) Lavallee, D. K.; Kopelove, A. B.; Anderson, O. P. *J. Am. Chem. Soc.* **1978**, *100*, 3025−3033.
(25) (a) Sugimoto, H.; Ueda, N.; Mori, M. *Bull. Chem. Soc. Jpn.* **1981**, *54*, 3425−3432. (b) Salehi, A.; Oertling, W. A.; Babcock, G. T.; Chang, C. K. *J. Am. Chem. Soc.* **1986**, *108*, 5630−5631.

unreacted free-base porphyrin. The filtrate was evaporated to dryness and then chromatographed on silica gel with $CH_2Cl_2$−acetone (40:1−10:1). The second red band was collected and then recrystallized from $CH_2Cl_2$−hexanes or $CH_2Cl_2$−$Et_2O$.

**(CH═CH-*Co,N′*)[(OEP)Co$^{III}$][(OEP)H$_2$]ClO$_4$ (5a).** Yield: 91% based on **1a**. $^1$H NMR ($CDCl_3$; $\delta$): 10.41, 9.06 (s × 2, 2H × 2, *meso*-H); 8.80 (s, 4H, *meso*-H); 4.64, 4.47, 3.29, 3.09 (m × 4, 2H × 4, −$CH_2$); 4.29, 3.96 (m × 2, 4H × 2, $CH_2$); 3.64 (m, 16H, $CH_2$); 2.13, 2.06, 1.81, 0.67 (t × 4, 6H × 4, $CH_3$); 1.55 (t, 24H, $CH_3$); −4.79 (d, 1H, Co−CH═, $J_{trans}$ = 11.7 Hz); −10.34 (d, 1H, N−CH═); −7.73 (br, 2H, NH). IR (KBr): 1090 cm$^{-1}$ ($ClO_4$). UV−vis ($CH_2Cl_2$) [$\lambda_{max}$ (log $\epsilon$)]: 383 (5.28), 515 (sh, 4.03), 551 (4.35), 587 (sh, 3.89), 611 (3.61) nm. Anal. Calcd for $C_{74}H_{92}N_8O_4ClCo$: C, 70.99; H, 7.41; N, 8.95. Found: C, 70.79; H, 7.28; N, 8.84.

**(CH═CH-*Co,N′*)[(OEP)Co$^{III}$][(TPP)H$_2$]ClO$_4$ (5b).** Yield: 89% based on **1a**. $^1$H NMR ($CDCl_3$; $\delta$): 9.06, 8.48 (d × 2, 2H × 2, pyrrole-$\beta$-H); 8.84, 6.82 (s × 2, 2H × 2, pyrrole-$\beta$-H); 9.11, 8.14 (d × 2, 2H × 2, outer phenyl-*o*-H); 8.29, 7.93 (t × 2, 2H × 2, outer phenyl-*m*-H); 8.05 (t, 2H, outer phenyl-*p*-H); 7.76 (t, 2H, inner phenyl-*p*-H); 7.63 (t, 4H, inner phenyl-*m*-H); 8.90 (s, 4H, *meso*-H); 3.49 (q, 16H, $CH_2$); 1.56 (t, 24H, $CH_3$); −3.08 (d, 1H, Co−CH═, $J_{trans}$ = 11.7 Hz); −9.66 (d, 1H, N−CH═). IR (KBr): 1090 cm$^{-1}$ ($ClO_4$). UV−vis ($CH_2Cl_2$) [$\lambda_{max}$ (log $\epsilon$)]: 391 (5.21), 443 (5.06), 515 (sh), 552 (4.28), 609 (3.95), 655 (3.97) nm. MALDI MS (dithranol): *m*/*e* 1234 ($M^+ + 2 - ClO_4$), 640 ((TPP)H + $C_2H_2$), 592 ((OEP)Co). Anal. Calcd for $C_{82}H_{76}N_8O_4ClCo•CH_2Cl_2•C_4H_{10}O$: C, 70.08; H, 5.95; N, 7.51. Found: C, 69.80; H, 5.80; N, 7.67.

**(CH═CH-*Co,N′*)[(OEP)Co$^{III}$][(TTP)H$_2$]ClO$_4$ (5c).** Yield: 89% based on **1a**. $^1$H NMR ($CDCl_3$; $\delta$): 8.89 (s, 4H, *meso*-H); 8.85, 6.79 (s × 2, 2H × 2, pyrrole-$\beta$-H); 9.08, 8.50 (d × 2, 2H × 2, pyrrole-$\beta$-H); 8.98, 8.09, 8.00, 7.74 (d × 4, 2H × 4, tolyl-*o*,*m*-H); 7.43, 7.23 (d × 2, 4H × 2, tolyl-*o*,*m*-H); 3.49 (m, 16H, $CH_2$); 2.90, 2.69 (s × 2, 6H × 2, tolyl-*p*-Me); 1.55 (t, 24H, $CH_3$); −3.16 (d, 1H, Co−CH═, $J_{trans}$ = 11.7 Hz); −9.65 (d, 1H, N−CH═). IR (KBr): 1090 cm$^{-1}$ ($ClO_4$). UV−vis ($CH_2Cl_2$) [$\lambda_{max}$ (log $\epsilon$)]: 389 (5.06), 446 (4.96), 515 (sh), 551 (4.17), 623 (3.94), 659 (3.97) nm. Anal. Calcd for $C_{74}H_{92}N_8O_4ClCo$: C, 70.99; H, 7.41; N, 8.95. Found: C, 70.79; H, 7.28; N, 8.84.

**(CH═CH-*Co,N′*)[(OEP)Co$^{III}$][N-Me(TTP)H]ClO$_4$ (5d).** Yield: 67% based on **1a**. $^1$H NMR ($CDCl_3$, 25 °C; $\delta$): 8.90, 8.90, 8.80, 8.40, 7.47, 6.72, 6.40, 6.34 (d × 8, 1H × 8, pyrrole-$\beta$-H); 9.03, 8.09, 7.89, 7.73 (d × 4, 1H × 4, aryl-H), 8.29, 8.16, 7.92, 7.60, 7.47, 7.47, 7.40, 6.23 (br, 1H × 8, aryl-H); 8.93 (s, 4H, *meso*-H); 3.49 (dq, 16H, $CH_2$); 1.53 (t, 24H, $CH_3$); 2.95, 2.89, 2.72, 2.71 (s × 4, 3H × 4, phenyl-*p*-Me); −3.62 (d, 1H, Co−CH═, $J_{trans}$ = 12.1 Hz); −9.24 (d, 1H, N−CH═); −4.75 (s, 1H, NH); −6.08 (s, 3H, N-Me). IR (KBr): 1090 cm$^{-1}$ ($ClO_4$). UV−vis ($CH_2Cl_2$) [$\lambda_{max}$ (log $\epsilon$)]: 388 (5.21), 457 (5.03), 551 (4.27), 644 (sh, 4.15), 687 (4.24) nm. Anal. Calcd for $C_{75}H_{94}N_8O_4ClCo$: C, 71.16; H, 7.48; N, 8.85. Found: C, 70.79; H, 7.28; N, 8.84.

**(CH═CH-*Co,N′*)[(TPP)Co$^{III}$][(OEP)H$_2$]ClO$_4$ (5e).** Yield: 49% based on **1b**. $^1$H NMR ($CDCl_3$; $\delta$): 10.21, 9.40 (s × 2, 2H × 2, *meso*-H); 8.06 (s, 8H, pyrrole-$\beta$-H); 8.0−7.6 (br, 8H, phenyl-*o*-H); 7.84 (t, 4H, phenyl-*p*-H); 7.53 (br, 8H, phenyl-*m*-H); 4.4−4.1 (m, 8H, $CH_2$); 3.83 (q, 4H, $CH_2$); 3.6−3.3 (m, 4H, $CH_2$); 1.92, 1.88, 1.59, 0.80 (t × 4, 6H × 4, $CH_3$); −3.87 (d, 1H, Co−CH═, $J_{trans}$ = 11.7 Hz); −9.60 (d, 1H, N−CH═); −7.48 (br, 2H, NH). IR (KBr): 1090 cm$^{-1}$ ($ClO_4$). UV−vis ($CH_2Cl_2$) [$\lambda_{max}$ (log $\epsilon$)]: 394 (5.61), 536 (4.52), 561 (sh, 4.39), 582 (sh, 4.25), 612 (3.90) nm. Anal. Calcd for $C_{82}H_{76}N_8O_4ClCo•{}^1/_2H_2O$: C, 73.45; H, 5.79; N, 8.36. Found: C, 73.36; H, 5.79; N, 8.35.

**(CH═CH-*Co,N′*)[(TTP)Co$^{III}$][(TTP)H$_2$]ClO$_4$ (5f).** Yield: 38% based on **1c**. $^1$H NMR ($CDCl_3$, at 0 °C; $\delta$): 8.86, 7.06 (s × 2, 2H × 2, pyrrole-$\beta$-H); 8.76, 8.51 (d × 2, 2H × 2, pyrrole-$\beta$-H); 8.05 (s, 8H, pyrrole-$\beta$-H); 8.24, 8.04, 7.77, 7.65 (d × 4, 2H × 4, tolyl-*o*,*m*-H); 7.93, 7.75, 7.53, 6.32 (broad d × 4, 2H × 4, tolyl-*o*,*m*-H); 7.45, 7.32, 7.24, 6.82 (d × 4, 4H × 4, tolyl-*o*,*m*-H); 2.83, 2.82 (s × 2, 6H × 2, tolyl-*p*-Me); 2.73 (s,12H, tolyl-*p*-Me); −2.25 (d, 1H, N−CH═, $J_{trans}$ = 12.0 Hz); −9.11 (d, 1H, Co−CH═). UV−vis ($CH_2Cl_2$) [$\lambda_{max}$ (log $\epsilon$)]: 415 (5.44), 448 (5.02), 532 (4.38), 562 (4.27), 666 (4.34) nm. Anal. Calcd for $C_{98}H_{76}N_8O_4ClCo$: C, 70.99; H, 7.41; N, 8.95. Found: C, 70.79; H, 7.28; N, 8.84.

**Vinylene-*Co,N′*-Linked Tris- and Tetrakis(porphyrin)s (9, 10).** A mixture of (CH═CH-*N,N′*)[(TTP)H]$_2$ (**8**) (0.05 mmol) and **1a** (0.11 mmol) was allowed to react under acetylene gas in $CH_2Cl_2$ (15 mL) for 3 h. Column chromatography on silica gel with $CH_2Cl_2$−acetone (20:1) gave a green brown band of the trimer, (CH═CH-*Co,N*$^{22′}$)-(CH═CH-*N*$^{21′}$,*N″*)[(OEP)Co$^{III}$][(TTP)H]$_2$ClO$_4$ (**9**), in a 26% yield after recrystallization. $^1$H NMR ($CDCl_3$; $\delta$): 8.97, 8.82, 8.75, 8.69, 8.54, 8.37, 8.07, 7.96, 7.64, 7.19, 6.44, 6.26, 6.06, 5.94, 5.91, 5.09 (d × 16, 1H × 16, pyrrole-$\beta$-H); 8.9−4.4 (m, tolyl-*o*,*m*-H); 8.54 (s, 4H, *meso*-H); 3.21 (m, 16H, $CH_2$); 2.98, 2.92, 2.83, 2.80, 2.77, 2.67, 2.53, 2.37 (s × 8, 3H × 8, tolyl-*p*-Me); 1.32 (t, 24H, $CH_3$); −4.38 (d, 1H, Co−CH═, $J_{trans}$ = 11.8 Hz); −5.68 (d, 1H, N−C═CH−N); −8.17 (d, 1H, N−CH═C−N); −10.62 (d, 1H, Co−C═CH−N); −3.8 (br, 1H, NH); −6.03 (s, 1H, NH). IR (KBr): 1090 cm$^{-1}$ ($ClO_4$). UV−vis ($CH_2Cl_2$) [$\lambda_{max}$ (log $\epsilon$)]: 389 (5.30), 431 (5.33), 475 (sh), 527 (4.16), 552 (4.32), 688 (4.23) nm. FAB MS (*p*-nitrobenzyl alcohol): *m*/*e* 2082 ($M^+$ + 1), 1983 ($M^+ + 1 - ClO_4$), 682 ((TTP)H + CH), 591 ((OEP)Co). Anal. Calcd for $C_{136}H_{122}N_{12}O_4ClCo•H_2O$: C, 73.60; H, 5.77; N, 7.57. Found: C, 73.56; H, 5.50; N, 7.71. A yellow brown band eluted with $CH_2Cl_2$−acetone (10:1) was collected and recrystallized from $CH_2Cl_2$−hexanes to afford a 62% yield of the tetramer, (CH═CH-*Co,N*$^{22′}$)-(CH═CH-*N*$^{21′}$,*N*$^{21″}$)(CH═CH-*N″*,*Co′*)[(OEP)Co$^{III}$]$_2$[(TTP)H]$_2$(ClO$_4$)$_2$ (**10**), as a mixture of two isomers. $^1$H NMR ($CDCl_3$) for one isomer: $\delta$ 9.1−4.0 (m, pyrrole-$\beta$-H and tolyl-*o*,*m*-H); 8.34 (s, 8H, *meso*-H); 3.00 (m, 32H, $CH_2$); 2.98, 2.86 (s × 2, 6H × 2, tolyl-*p*-Me); 2.56 (s, 12H, tolyl-*p*-Me); 1.16 (t, 48H, $CH_3$); −4.84 (d, 2H, Co−CH═, $J_{trans}$ = 11.9 Hz); −6.28 (s, 2H, N−CH═CH−N); −11.21 (d, 2H, Co−C═CH−N); −7.77 (s, 2H, NH). $^1$H NMR ($CDCl_3$) for the other isomer: $\delta$ 9.1−4.0 (m, pyrrole-$\beta$-H and tolyl-*o*,*m*-H); 8.33 (s, 8H, *meso*-H); 3.00 (m, 32H, $CH_2$); 2.80, 2.65 (s × 2, 6H × 2, tolyl-*p*-Me); 2.30 (s, 12H, tolyl-*p*-Me); 1.19 (t, 48H, $CH_3$); −4.75 (d, 2H, Co−CH═, $J_{trans}$ = 11.9 Hz); −6.19 (s, 2H, N−CH═CH−N); −11.28 (d, 2H, Co−C═CH−N); −7.38 (s, 2H, NH). IR (KBr): 1090 cm$^{-1}$ ($ClO_4$). UV−vis ($CH_2Cl_2$) ($\lambda_{max}$): 388, 458, 552, 680 nm. FAB MS (*p*-nitrobenzyl alcohol): *m*/*e* 2700 ($M^+ + 2 - ClO_4$), 2600 ($M^+ + 1 - 2ClO_4$), 1983 ($M^+ + 1 - 2ClO_4$ − (OEP)Co − $C_2H_2$), 1391 ($M^+ + 1 - 2ClO_4$ − 2(OEP)Co − $C_2H_2$), 1365 ($M^+ - 2ClO_4$ − 2(OEP)Co − $2C_2H_2$), 1301 (($M^{2+}$ + 2 − $2ClO_4$)/2), 682 ((TTP)H + CH), 591 ((OEP)Co). Anal. Calcd for $C_{174}H_{168}N_{16}O_8Cl_2Co_2$: C, 74.64; H, 6.05; N, 8.00. Found: C, 74.85; H, 6.25; N, 7.90.

**Vinylene-*N,N′*-Linked Co$^{II}$ Multi(porphyrin)s (11b,c,e, 12). General Procedure.** A mixture of the complex **5b** (0.12 mmol) and $Fe(ClO_4)_3•6H_2O$ (0.50 mmol) in 60 mL of $CH_2Cl_2$ was stirred for 2 h in an ice bath. When the Soret band of **5b** at 391 nm had gone, the reaction mixture was filtered to remove inorganic iron salts. Saturated NaCl solution (100 mL) was then added, and the stirring was continued for a further 2 h. After an aqueous layer was separated off, an organic layer was washed with $H_2O$ and then with a 1% aqueous $Na_2CO_3$ solution. The $CH_2Cl_2$ solution was dried over $Na_2SO_4$, condensed, and chromatographed on silica gel. The band eluted with $CH_2Cl_2$−acetone (20:1) was collected. Recrystallization from $CH_2Cl_2$−hexanes gave red crystals of Co$^{II}$ complexes of vinylene-*N,N′*-linked multi(porphyrin)s.

**(CH═CH-*N,N′*)[(OEP)Co$^{II}$Cl][(TPP)H] (11b).** Yield: 82%. $^1$H NMR ($CDCl_3$; $\delta$): 36.6, 26.9, 23.3, 20.4, 19.2, 19.0, 14.0, 13.8 (s × 8, 2H × 8, $CH_2$); 13.9, −10.8 (s × 2, 2H × 2, *meso*-H); 9.9, 8.2, 2.7, 0.7 (s × 4, 6H × 4, $CH_3$); 9.9, 4.7 (s × 2, 2H × 2, inner phenyl-*o*-H); 6.35, 4.80 (s × 2, 2H × 2, outer phenyl-*o*-H); 14.8, 7.7 (s × 2, 2H × 2, inner phenyl-*m*-H); 7.50, 6.40 (s × 2, 2H × 2, outer phenyl-*m*-H); 10.0 (s, 2H, inner phenyl-*p*-H); 7.17 (s, 2H, outer phenyl-*p*-H); 5.7, 5.5, 5.3, 3.0 (s × 4, 2H × 4, pyrrole-$\beta$-H); −20.7 (s, 1H, NH); −78.2 (s, 1H, N−CH═); −106 (br, 1H, Co−N−CH═). UV−vis ($CH_2Cl_2$) [$\lambda_{max}$ (log $\epsilon$)]: 426 (5.30), 536 (4.11), 574 (4.26), 681 (3.65) nm. MALDI MS (dithranol): *m*/*e* 1267 ($M^+$ + 1), 640 ((TPP)H + $C_2H_2$), 592 ((OEP)Co). Anal. Calcd for $C_{82}H_{75}N_8ClCo$: C, 77.74; H, 5.97; N, 8.84. Found: C, 77.68; H, 6.06; N, 8.82.

**(CH═CH-*N,N′*)[(OEP)Co$^{II}$Cl][(TTP)H] (11c).** Recrystallization from $CH_2Cl_2$−$Et_2O$ gave crystals of **11c** in a 80% yield. $^1$H NMR ($CDCl_3$; $\delta$): 36.4, 26.8, 23.2, 20.3, 19.0, 18.7, 13.8, 13.4 (s × 8, 2H × 8, $CH_2$); 13.0, −10.6 (s × 2, 2H × 2, *meso*-H); 9.9, 8.3, 2.8, 0.7 (s × 4, 6H × 4, $CH_3$); 4.85, 2.33 (s × 2, 6H × 2, tolyl-*p*-Me); 9.8, 4.6

(s × 2, 2H × 2, inner phenyl-*o*-H); 6.24, 4.69 (s × 2, 2H × 2, outer phenyl-*o*-H); 14.5, 7.5 (s × 2, 2H × 2, inner phenyl-*m*-H); 7.28, 6.21 (s × 2, 2H × 2, outer phenyl-*m*-H); 5.7, 5.5, 5.3, 2.8 (s × 4, 2H × 4, pyrrole-$\beta$-H); −20.7 (s, 1H, NH); −78.0 (s, 1H, N−CH═); −106 (br, 1H, Co−N−CH═). UV−vis ($CH_2Cl_2$) [$\lambda_{max}$ (log $\epsilon$)]: 428 (5.52), 540 (4.37), 580 (4.59), 685 (3.97) nm. Anal. Calcd for $C_{86}H_{83}N_8ClCo$: C, 78.07; H, 6.32; N, 8.47. Found: C, 78.11; H, 6.53; N, 8.49.

**(CH═CH-*N*,*N*′)[(TPP)Co$^{II}$Cl][(OEP)H$_2$]Cl (11e).** A mixture of **5e** (0.026 mmol) and $FeCl_3$ (0.24 mmol) in 20 mL of $CH_2Cl_2$ was stirred for 20 min at 30 °C under argon. Saturated NaCl solution (20 mL) was then added, and the stirring was continued for a further 1 h. After the aqueous layer was separated off, the organic layer was washed with $H_2O$, dried over $Na_2SO_4$, condensed, and chromatographed on silica gel. The green band eluted with $CH_2Cl_2$−MeOH (10:1) was collected, and recrystallization from $CH_2Cl_2$−$Et_2O$ gave green crystals of **11e** in a 53% yield. $^1$H NMR ($CDCl_3$; $\delta$): 49.3, 43.9, 39.1, −6.6 (s × 4, 2H × 4, pyrrole-$\beta$-H); 23.5, 19.6, 4.1, −9.9 (s × 4, 2H × 4, phenyl-*o*-H); 13.6, 12.5, 7.3, 6.0 (s × 4, 2H × 4, phenyl-*m*-H); 9.6, 6.6 (s × 2, 2H × 2, phenyl-*p*-H); 13.1, 1.3, 0.0, −0.8 (s × 4, 6H × 4, $CH_3$); 8.6, 7.2, 4.7, 3.4 (s × 4, 2H × 4, $CH_2$); 1.7, 1.0 (s × 2, 4H × 2, $CH_2$); 6.7, 4.9 (s × 2, 2H × 2, *meso*-H); −86.2 (s, 1H, N−CH═); −113 (br, 1H, Co−N−CH═). UV−vis ($CH_2Cl_2$) [$\lambda_{max}$ (log $\epsilon$)]: 395 (5.25), 447 (4.90), 543 (sh, 4.04), 564 (4.18), 585 (4.05), 610 (4.04), 670 (3.71) nm. Anal. Calcd for $C_{82}H_{76}N_8Cl_2Co$: C, 75.56; H, 5.88; N, 8.60. Found: C, 75.32; H, 5.93; N, 8.41.

**(CH═CH-$N_{OEP}$,$N^{21'}$)(CH═CH-$N^{21'}$,$N''$)[(OEP)Co$^{II}$Cl]-[(TTP)H]$_2$Cl (12).** $Fe(ClO_4)_3$•$6H_2O$ (0.17 mmol) was added to a $CH_2Cl_2$ (10 mL) solution of complex **9** (0.023 mmol). The reaction mixture was stirred in an ice bath until the Soret band at 389 nm disappeared. After the reaction mixture was treated with saturated NaCl aqueous solution as in the case of **11e**, recrystallization from $CH_2Cl_2$−$Et_2O$ gave **12** in a 69% yield. $^1$H NMR ($CDCl_3$; $\delta$): 36.9, 36.1, 26.7, 26.3, 24.6, 22.3, 21.3, 21.3, 20.8, 20.8, 20.6, 17.3, 15.6, 12.5, 12.1, 11.1 (s × 16, 1H × 16, $CH_2$); 27.1 to −3.8 (pyrrole-$\beta$-H and tolyl-*o*,*m*-H); 13.0, 10.2, −11.0, −11.3 (s × 4, 1H × 4, *meso*-H); 9.6, 9.4, 8.8, 7.8, 5.7, 3.4, −0.2, −0.6 (s, 3H × 8, $CH_3$); 6.31, 3.84, 3.18, 2.54, 2.54, 2.12, 1.96, 1.93 (s × 8, 3H × 8, tolyl-*p*-Me); −7.83 (s, 1H, N″H); −22.7 (s, 1H, N′H); −13.0 (d, 1H, $N^{21'}$-C═CH−N″, $J_{trans}$ = 11.9 Hz); −20.9 (d, 1H, $N^{21'}$-CH═C−N″); −88.5 (s, 1H, $N_{OEP}$−C═CH−$N^{22'}$); −117 (br, 1H, $N_{OEP}$−CH═). UV−vis ($CH_2Cl_2$) [$\lambda_{max}$ (log $\epsilon$)]: 426 (5.50), 477 (4.63), 530 (4.23), 577 (4.32), 632 (4.15), 688 (4.33) nm. MALDI MS (dithranol): *m*/*e* 2022 ($M^+$ + 5 − Cl), 696 ((TTP)$H_2$ + $C_2H_2$), 683 ((TTP)$H_2$ + CH), 591 ((OEP)Co), 560 ((OEP)$H_2$ + $C_2H_2$), 547 ((OEP)-$H_2$ + CH). Anal. Calcd for $C_{136}H_{122}N_{12}Cl_2Co$•$H_2O$•$CH_2Cl_2$: C, 76.27; H, 5.88; N, 7.79. Found: C, 76.41; H, 5.88; N, 7.67.

**Metal-Free Vinylene-*N*,*N*′-Linked Bis(porphyrin)s (13a−c). (CH═CH-*N*,*N*′)[(OEP)H$_2$]$_2$(ClO$_4$)$_2$ (13a).** A mixture of a $CH_2Cl_2$ (10 mL) solution of **5a** (0.081 mmol) and a 60% $HClO_4$ aqueous solution (10 mL) was vigorously stirred overnight. The organic layer was separated, washed with water, and then dried over $Na_2SO_4$. Recrystallization from $CH_2Cl_2$−$Et_2O$ gave **13a** in a 90% yield. $^1$H NMR ($CDCl_3$; $\delta$): 10.40, 8.77 (s × 2, 4H × 2, *meso*-H); 4.28, 3.94, 3.79 (m × 3, 4H × 3, $CH_2$); 4.2 (m, 12H, $CH_2$); 3.00 (m, 8H, $CH_2$); 2.05, 1.98, 1.67, 0.68 (t × 4, 12H × 4, $CH_3$); −7.69 (br, 4H, NH); −8.40 (s, 2H, N−CH═). UV−vis ($CH_2Cl_2$) [$\lambda_{max}$ (log $\epsilon$)]: 388 (5.41), 542 (sh), 562 (4.27), 586 (sh), 611 (3.90) nm. IR (KBr): 1120 cm$^{-1}$ ($ClO_4$). FAB MS (*p*-nitrobenzyl alcohol): *m*/*e* 1194 ($M^+$ − $ClO_4$), 1095 ($M^+$ − 2$ClO_4$). Anal. Calcd for $C_{74}H_{94}N_8O_8Cl_2$•$CH_2Cl_2$: C, 65.30; H, 7.01; N, 8.12. Found: C, 64.83; H, 7.11; N, 8.49.

**(CH═CH-*N*,*N*′)[(OEP)H][(TPP)H] (13b).** The complex **11b** (0.088 mmol) was dissolved in $CH_2Cl_2$ (40 mL) containing trifluoroacetic acid (5 mL), and the mixture was stirred at room temperature for 30 min. This acidic $CH_2Cl_2$ solution was neutralized with 28% aqueous ammonia when an initial green color turned red. The organic layer was separated and dried over $Na_2SO_4$. Chromatography on aluminum oxide using $CH_2Cl_2$−acetone (20:1) followed by recrystallization from $CH_2Cl_2$−hexanes gave **13b** in an 85% yield. $^1$H NMR ($CDCl_3$; $\delta$): 9.78, 8.06 (s × 2, 2H × 2, *meso*-H); 4.4−2.4 (m, 16H, $CH_2$); 2.02, 1.73, 1.37, 0.53 (t × 4, 6H × 4, $CH_3$); 8.88, 5.97 (s × 2, 2H × 2, pyrrole-$\beta$-H); 8.50, 8.19 (d × 2, 2H × 2, pyrrole-$\beta$-H, $J$ = 4.0 Hz); 8.74 (d, 2H, phenyl-*o*-H); 8.1−7.4 (m, phenyl-H); −4.44 (br, 1H, $N_{OEP}$H); −5.83 (d, 1H, N′−CH═, $J_{trans}$ = 12.3 Hz); −6.45 (d, 1H, $N_{OEP}$−CH═). UV−vis ($CH_2Cl_2$) [$\lambda_{max}$ (log $\epsilon$)]: 402 (5.29), 436 (5.07), 506 (4.11), 536 (4.15), 578 (4.18), 620 (3.70), 647 (3.41), 682 (3.60) nm. Anal. Calcd for $C_{82}H_{76}N_8$•$2H_2O$•$CH_2Cl_2$: C, 77.01; H, 6.38; N, 8.66. Found: C, 77.03; H, 6.62; N, 8.82.

**(CH═CH-*N*,*N*′)[(OEP)H][(TTP)H] (13c).** Yield: 89% based on **11c**. $^1$H NMR ($CDCl_3$; $\delta$): 9.75, 7.93 (s × 2, 2H × 2, *meso*-H); 4.4−2.4 (m, 16H, $CH_2$); 2.03, 1.72, 1.36, 0.51 (t × 4, 6H × 4, $CH_3$); 8.87, 5.95 (s × 2, 2H × 2, pyrrole-$\beta$-H); 8.49, 8.18 (d × 2, 2H × 2, pyrrole-$\beta$-H, $J$ = 4.0 Hz); 8.7−7.2 (m, phenyl-H); 2.80, 2.63 (s × 2, 6H × 2, tolyl-*p*-Me); −3.1 (br, 1H, N′H); −4.31 (s, 1H, $N_{OEP}$H); −5.87 (d, 1H, N′−CH═, $J_{trans}$ = 12.4 Hz); −6.40 (d, 1H, $N_{OEP}$−CH═). UV−vis ($CH_2Cl_2$) [$\lambda_{max}$ (log $\epsilon$)]: 400 (5.25), 440 (4.99), 506 (3.99), 536 (4.01), 583 (4.13), 685 (3.57) nm. Anal. Calcd for $C_{86}H_{84}N_8$•$3H_2O$: C, 80.46; H, 7.07; N, 8.73. Found: C, 80.61; H, 7.06; N, 8.74.

**Homo- and Heterobimetallic Vinylene-*N*,*N*′-Linked Bis(porphyrin)s (14a−c, 15a,b). (CH═CH-*N*,*N*′)[(OEP)Co$^{II}$Cl][(TPP)Co$^{II}$Cl] (14a).** A mixture of **13b** (0.027 mmol) in $CH_2Cl_2$ (10 mL), Co(OAc)$_2$•$4H_2O$ (0.27 mmol) in MeOH (10 mL), and 2,6-lutidine (0.27 mmol) was stirred at room temperature for 20 min. Then, a saturated aqueous NaCl solution (20 mL) was added and the mixture was stirred for 1 h. The organic layer was separated, washed with water, and dried over anhydrous $Na_2SO_4$. A green band eluted from column chromatography on silica gel with $CH_2Cl_2$−acetone (40:1) was recrystallized from $CH_2Cl_2$−$Et_2O$ to give a 59% yield of **14a**. $^1$H NMR ($CDCl_3$; $\delta$): 7.7, −13.2 (s × 2, 2H × 2, *meso*-H); 34.2, 25.6, 24.0, 21.7, 19.2, 17.0, 17.0, 15.4 (s × 8, 2H × 8, $CH_2$); 13.2, 7.4, 7.4, −2.2 (s × 4, 6H × 4, $CH_3$); 45.0, 39.0, 36.4, −8.7 (s × 4, 2H × 4, pyrrole-$\beta$-H); 20.0, 16.7, 0.2 (s × 3, 2H × 3, phenyl-*o*-H; the fourth signal was not detected); 14.2, 13.6, 11.6, 5.8 (s × 4, 2H × 4, phenyl-*m*-H); 9.5, 8.5 (s × 2, 2H × 2, phenyl-*p*-H); −182 (br, 2H, N−CH═). UV−vis ($CH_2Cl_2$) [$\lambda_{max}$ (log $\epsilon$)]: 444 (5.24), 568 (3.97), 603 (4.14), 662 (3.89) nm. Anal. Calcd for $C_{82}H_{74}N_8Cl_2Co_2$•$4H_2O$: C, 68.76; H, 5.77; N, 7.82. Found: C, 68.31; H, 5.89; N, 7.57.

**(CH═CH-*N*,*N*′)[(OEP)Cu$^{II}$Cl][(TPP)Cu$^{II}$Cl] (14b).** A mixture of **13b** (0.024 mmol) in $CH_2Cl_2$ (5 mL), $CuCl_2$•$2H_2O$ (0.072 mmol) in MeOH (5 mL), and 2,6-lutidine (0.072 mmol) was stirred at room temperature for 30 min. The solvent was removed, and the residue was chromatographed on silica gel with $CH_2Cl_2$−acetone (20:1). The green fraction was recrystallized from $CH_2Cl_2$−$Et_2O$ to give a 75% yield of **14b**. UV−vis ($CH_2Cl_2$) [$\lambda_{max}$ (log $\epsilon$)]: 389 (5.01), 413 (4.98), 456 (4.92), 577 (4.10), 611 (4.03), 675 (3.82) nm. Anal. Calcd for $C_{82}H_{74}N_8Cl_2Cu_2$•$CH_2Cl_2$•$H_2O$: C, 67.70; H, 5.34; N, 7.61. Found: C, 67.74; H, 5.27; N, 7.71.

**(CH═CH-*N*,*N*′)[(OEP)Zn$^{II}$Cl][(TPP)Zn$^{II}$Cl] (14c).** To the compound **13b** (0.016 mmol) in 20 mL of $CH_2Cl_2$ was added Zn(OAc)$_2$•$2H_2O$ (0.48 mmol) in MeOH (10 mL) and 2,6-lutidine (0.48 mmol). The whole mixture was stirred at room temperature for 15 min. Then, a saturated aqueous NaCl solution (20 mL) was added and the mixture was stirred for 1 h. An organic layer was separated, washed with water, and dried over anhydrous $Na_2SO_4$. A green band eluted from column chromatography on silica gel with $CH_2Cl_2$−acetone (40:1) was recrystallized from $CH_2Cl_2$−$Et_2O$ to give an 82% yield of **14c**. $^1$H NMR ($CDCl_3$; $\delta$): 10.15, 8.43 (s × 2, 2H × 2, *meso*-H); 4.4−2.4 (m, 16H, $CH_2$); 2.08, 1.90, 1.54, 0.30 (t × 4, 6H × 4, $CH_3$); 8.94, 6.55 (s × 2, 2H × 2, pyrrole-$\beta$-H); 8.88, 8.40 (d × 2, 2H × 2, pyrrole-$\beta$-H, $J$ = 4.8 Hz); 8.56, 8.18, 7.53, 5.15 (d × 4, 2H × 4, phenyl-*o*-H); 8.03, 7.81, 7.47, 7.37 (t × 4, 2H × 4, phenyl-*m*-H); 7.92, 7.61 (t × 2, 2H × 2, phenyl-*p*-H); −6.30, −6.41 (d × 2, 1H × 2, N−CH═, $J_{trans}$ = 12.5 Hz). UV−vis ($CH_2Cl_2$) [$\lambda_{max}$ (log $\epsilon$)]: 426 (5.38), 577 (4.17), 596 (4.29), 621 (4.07), 664 (3.90) nm. Anal. Calcd for $C_{82}H_{74}$-$N_8Cl_2Zn_2$•$H_2O$: C, 70.79; H, 5.51; N, 8.05. Found: C, 70.46; H, 5.77; N, 7.93.

**(CH═CH-*N*,*N*′)[(OEP)Co$^{II}$Cl][(TPP)Cu$^{II}$Cl] (15a).** A mixture of the complex **11b** (0.022 mmol) in $CH_2Cl_2$ (4 mL), Cu($ClO_4$)•$6H_2O$ (0.028 mmol) in MeOH (4 mL), and 2,6-lutidine (0.028 mmol) was stirred at room temperature for 20 min. Then, a saturated aqueous NaCl solution (20 mL) was added and the mixture was stirred for 1 h. The organic layer was separated, washed with water, and dried over anhydrous $Na_2SO_4$. A green band eluted from column chromatography on silica gel with $CH_2Cl_2$−acetone (20:1) was recrystallized from $CH_2$-

$Cl_2-Et_2O$ to give a 75% yield of **15a**. $^1H$ NMR ($CDCl_3$; $\delta$): −9.7, 13.0 (s × 2, 2H × 2, *meso*-H); 37.3, 27.0, 22.9, 20.5, 20.5, 19.8, 15.2, 15.2 (s × 8, 2H × 8, $CH_2$); 9.9, 7.8, 0.3, −1.0 (s × 4, 6H × 4, $CH_3$); 43, −3.5 (br, pyrrole-$\beta$-H); 17.8, 4.0, 4.0, 3.2 (broad s × 4, 2H × 4, phenyl-*o*-H); 15.7, 7.4, 6.8, 6.1 (s × 4, 2H × 4, phenyl-*m*-H); 10.2, 6.7 (s × 2, 2H × 2, phenyl-*p*-H); ca. −80 (br, $N_{TPP}-CH=$); −106 (br, 1H, $N_{OEP}-CH=$). UV−vis ($CH_2Cl_2$) [$\lambda_{max}$ (log $\epsilon$)]: 393 (sh, 4.96), 434 (5.10), 590 (4.16), 597 (4.16), 673 (3.80) nm. Anal. Calcd for $C_{82}H_{74}N_8Cl_2CoCu\bullet CH_2Cl_2$: C, 68.76; H, 5.28; N, 7.73. Found: C, 68.38; H, 5.50; N, 7.98.

**(CH=CH-*N,N′*)[(OEP)Co$^{II}$Cl][(TPP)Zn$^{II}$Cl] (15b).** A mixture of the complex **11b** (0.026 mmol) in $CH_2Cl_2$ (4 mL), $ZnCl_2$ (0.034 mmol) in MeOH (1 mL), and 2,6-lutidine (0.034 mmol) was stirred at room temperature for 30 min. The solvent was removed, and the residue was chromatographed on silica gel with $CH_2Cl_2$−acetone (40:1). The green fraction was recrystallized from $CH_2Cl_2-Et_2O$ to give an 88% yield of **15b**. $^1H$ NMR ($CDCl_3$; $\delta$): 12.7, −9.9 (s × 2, 2H × 2, *meso*-H); 37.2, 26.8, 22.7, 20.2, 20.2, 19.9, 15.0, 15.0 (s × 8, 2H × 8, $CH_2$); 9.6, 7.8, 0.4, −1.1 (s × 4, 6H × 4, $CH_3$); 5.4, 5.4, 5.0, 4.5 (s × 4, 2H × 4, pyrrole-$\beta$-H); 15.5, 5.5, 4.8, 4.6 (s × 4, 2H × 4, phenyl-*o*-H); 15.7, 7.8, 7.2, 6.2 (s × 4, 2H × 4, phenyl-*m*-H); 10.3, 6.9 (s × 2, 2H × 2, phenyl-*p*-H); −85.4 (s, 1H, $N_{TPP}-CH=$); −109.5 (br, 1H, $N_{OEP}-CH=$). UV−vis ($CH_2Cl_2$) [$\lambda_{max}$ (log $\epsilon$)]: 439 (5.29), 568 (4.03), 603 (4.19), 663 (3.84) nm. Anal. Calcd for $C_{82}H_{74}N_8Cl_2CoZn\bullet 2H_2O$: C, 70.21; H, 5.60; N, 7.99. Found: C, 69.80; H, 5.50; N, 7.70.

**Single-Crystal X-ray Structure Determination of 15b.** A black crystal of (CH=CH-*N,N′*)[(OEP)Co$^{II}$Cl][(TPP)Zn$^{II}$Cl] (**15b**) was obtained by recrystallization from $CH_2Cl_2-Et_2O$. All measurements were made on a Rigaku AFC5R automated four-circle diffractometer using graphite-monochromated Mo K$\alpha$ radiation ($\lambda$ = 0.710 69 Å). As most of the high-angle cell reflections ($22 < 2\theta < 25°$) were weak, the unit cell parameters were obtained from least-squares refinements of 20 reflections ($7.4 < 2\theta < 15.0°$). The intensities of three representative reflections which were measured after every 150 reflections showed a 0.82% increase during data collection. The data were corrected for Lorentz and polarization effects and absorption based on azimuthal scans. The refined cell parameters and relevant crystal data are summarized in Table 2. The structure was solved by direct methods and refined by the full-matrix least-squares method (Texsan[26]) on a Hewlett-Packard 712-60 work station. All non-hydrogen atoms in the main porphyrin rings were unequivocally found by successive difference Fourier syntheses and least-squares refinements. Two ethyl groups of the OEP ligand were found to be disordered toward the Zn(TPP) and the opposite directions with occupancies of 0.7 [the C(23)C(24) and C(29)C(30) ethyl groups] and 0.3 [the C(23)C(24′) and C(29′)C(30′) ethyl groups], respectively. The $^1H$ NMR spectrum of **15b** indicated existence of a solvate $CH_2Cl_2$ molecule per one molecule of **15b** in the crystal. Solvate $CH_2Cl_2$ molecules were found in two different positions with 0.7 [C(83)CL(3)CL(4) and C(83)CL(3′)CL(4′)] and 0.3 [C(84)CL(5)CL(6)] occupancies. The former $CH_2Cl_2$ is disordered with 0.4 and 0.3 occupancies. Non-hydrogen atoms of $CH_2Cl_2$ were refined isotropically, while non-hydrogen atoms of the metalloporphyrin were refined anisotropically.

All hydrogen atom positions were calculated by assuming idealized geometries and the C−H distance of 0.95 Å. Their contributions were added to the structure factor calculations, but their parameters were not refined.

Neutral atom scattering factors were taken from Cromer and Waber.[27] Anomalous dispersion effects were included in $F_c$; the values for $\Delta f'$ and $\Delta f''$ were those of Cromer.[28] The atomic coordinates with *B*(eq), *U* values, bond distances, bond angles, torsional angles, least-squares planes, and an ORTEP drawing are given in Tables II−VII and Figure 1, respectively, in the Supporting Information.

**Acknowledgment.** This work was supported by a Grant-in-Aid for Scientific Research from the Ministry of Education, Science, Sports, and Culture of Japan. A part of this work was performed for the Photonics Material Laboratory of the Graduate School of Science and Technology of Kobe University. We are grateful to Nichigo Acetylene Co. Ltd. (Osaka, Japan) for a gift of extra pure grade acetylene gas, to Ms. S. Nomura (IMS) for FABMS analysis, and to Ms. M. Nishinaka (Kobe University) for microanalysis.

**Supporting Information Available:** Full listings of data pertinent to the crystal structure determination, including atomic coordinates, isotropic and anisotropic thermal parameters, bond distances, bond angles, torsion angles, and least-squares planes, and an ORTEP drawing (24 pages). Ordering information is given on any current masthead page.

IC970770K

(26) *TEXSAN-TEXRAY Structure Analysis Package*; Molecular Structure Corp.: The Woodlands, TX, 1985.

(27) Cromer, D. T.; Waber, J. T. *International Tables for X-ray Crystallography*; The Kynoch Press: Birmingham, England, 1974; Vol. IV, Table 2.2A.

(28) Cromer, D. T.; Waber, J. T. *International Tables for X-ray Crystallography*; The Kynoch Press: Birmingham, England, 1974; Vol. IV, Table 2.3.1.